Methodology for measurements of electrical conductivity of doped silicon carbide

by

Nils-Bertil Frisk, Douglas Jutsell Nilsson

Diploma work No. 137/2014
at Department of Materials and Manufacturing Technology
Division of High Voltage Engineering
Chalmers University of Technology
Gothenburg, Sweden

Diploma work in the Master programme Electrical Power Engineering

Performed at: Chalmers University of Technology
SE-412 96 Gothenburg
Sweden

Supervisor/Examiner: Associate Professor Yuriy Serdyuk
Department of Materials and Manufacturing Technology
Division of High Voltage Engineering
Chalmers University of Technology
SE-412 96 Gothenburg
Sweden

Methodology for measurements of electrical conductivity of doped silicon carbide
Nils-Bertil Frisk, Douglas Jutsell Nilsson

Technical report no 137/2014
Department of Materials and Manufacturing Technology
Division of High Voltage Engineering
Chalmers University of Technology
SE-412 96 Gothenburg
Sweden
Telephone + 46 (0)31-772 1000

Chalmers Reproservice
Gothenburg, Sweden 2014

Methodology for measurements of electrical conductivity of doped silicon carbide

Nils-Bertil Frisk, Douglas Jutsell Nilsson
Department of Materials and Manufacturing Technology
Division of High Voltage Engineering
Chalmers University of Technology

Summary

This work aims to develop a method for measurements of electric conductivity of doped silicon carbide in powder form. A general purpose measurement cell is used to produce an array of initial results and the experience and conclusions drawn from those are used to refine both the hardware and methodology. The main part of the refinements are focused on how force is applied to the powder and temperature control. The developed method is used to compare and evaluate produced batches of the material. The work concludes with a series of measurements that quantifies the repeatability of the final system together with ideas and suggestions for how the result could be improved.

Keywords: silicon carbide, powder, repeatability, electric conductivity

Table of contents

1 Introduction

1.1 Background

Silicon carbide, SiC, is used as an admixture in insulating polymers such as epoxy and silicon rubber. These are base materials for producing high voltage cable accessories, in particular, cable terminations and joints. It provides non-linear electric properties for the composite materials that are vital for electric field grading in HVDC applications. To insure the performance of the final product, the field dependent conductivity of SiC powder needs to be monitored during the material preparation process. Currently, there is no well-established procedure for measuring powder conductivity which provides satisfactory accuracy and repeatability of the results.

1.2 Aim

The goal of the work is to develop a procedure for measuring the electric conductivity of SiC powder that can be used to compare the conductivity of one produced quantity to that of another. The main requirements of the system is repeatability of the measurements within a given range of accuracy and a reasonably short measuring time.

1.3 Method and scope

Experimental studies are to be conducted to evaluate existing measuring techniques within the time- and frequency domains using a specially developed test cell for electric characterization of materials. Further, a set of experiments is to be carried out with the chosen method to analyze the influence of several factors on the accuracy and repeatability of the results. In particular, environmental and physical conditions of the powder during measurements are to be investigated.

2 Theory

2.1 Dielectric response

This section presents the basics of dielectric measurements and is based on the theories described in [1].

2.1.1 Time Domain

If an electric field is applied to a dielectric material, a displacement current is released to maintain the area charge density at the electrodes and in dielectric materials within the sample. This is called polarization and is governed by the equation

$$\boldsymbol{P}(t) = \boldsymbol{D}(t) - \epsilon_0 \boldsymbol{E}(t) \tag{1}$$

If $\boldsymbol{E}(t)$ is considered to be a step function there is a time delay between $\boldsymbol{P}(t)$ and $\boldsymbol{E}(t)$ which can be described by the dielectric materials susceptibility $\chi(t)$. The polarization can then be expressed as

$$\boldsymbol{P}(t) = \epsilon_0 \chi(0)\, \boldsymbol{E}(t) + \epsilon_0 \int_0^t \boldsymbol{E}(\tau) \frac{\mathrm{d}f(t-\tau)}{\mathrm{d}t} \mathrm{d}\tau, \tag{2}$$

where $f(t) = \frac{\mathrm{d}\chi(t)}{\mathrm{d}t}$ and an ideal step excitation gives $\chi(0) = 0$. However, in actual measurements a time delay will be present and a susceptibility $\chi(0')$. The polarization is a slow process in comparison to $\boldsymbol{E}(t)$ and contributes to the main part of the displacement current in a test object. The density of the total current in a material can be written as

$$\boldsymbol{J}(t) = \sigma_{\mathrm{DC}} \boldsymbol{E}(t) + \frac{\mathrm{d}\boldsymbol{D}(t)}{\mathrm{d}t}, \tag{3}$$

where σ_{DC} is the effective DC-conductivity of the material and $\frac{\mathrm{d}\boldsymbol{D}(t)}{\mathrm{d}t}$ is the change in the displacement current. If t$\rightarrow \infty$ then $\frac{\mathrm{d}\boldsymbol{D}(t)}{\mathrm{d}t} \rightarrow 0$ and only the $\sigma_{\mathrm{DC}}\boldsymbol{E}(t)$ will be left. However, in practice this may take an extremely long time. By studying the depolarization current and using superposition, the displacement current can be removed and only the conductive one will be left as illustrated in Figure 1. This method is applicable to dielectrics, and may not apply to other materials in the same extent.

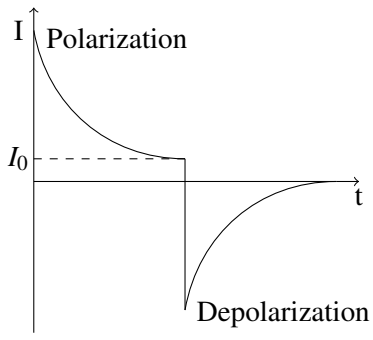

Figure 1: Polarization and depolarization should be equal in area and can be removed by superposition to get a value for the pure DC-conductivity. I_0 is the pure DC current sought.

2.1.2 Frequency domain

In the frequency domain polarization must be even more carefully considered, because it will occur every half cycle. By replacing the current density in eq 3 with the polarization expression in eq 2 and with eq 1 the conduction can be expressed as

$$\boldsymbol{J}(t) = \sigma_{\mathrm{DC}}\boldsymbol{E}(t) + \epsilon_0\left(1+\chi\left(0'\right)\right)\frac{\mathrm{d}\boldsymbol{E}(t)}{\mathrm{d}t} + \epsilon_0\frac{\mathrm{d}}{\mathrm{d}t}\int_{0'}^{t}\boldsymbol{E}(\tau)\frac{\mathrm{d}f(t-\tau)}{\mathrm{d}t}\mathrm{d}\tau, \tag{4}$$

using Fourier transformation this expression can be written as

$$\boldsymbol{J}(\omega) = \boldsymbol{E}(\omega)\left[\sigma_{\mathrm{DC}} + \mathrm{j}\omega\epsilon_0\left(1+\boldsymbol{F}(\omega)\right)\right] \tag{5}$$

where $\boldsymbol{F}(\omega) = \chi'(\omega) - \mathrm{j}\chi''(\omega)$, that results in a real and imaginary parts as

$$\boldsymbol{J}(\omega) = \left[\sigma_{\mathrm{DC}} + \omega\epsilon_0\chi''(\omega) + \mathrm{j}\omega\epsilon_0\left(1+\chi'(\omega)\right)\right]\boldsymbol{E}(\omega) \tag{6}$$

Here, the quantity

$$\epsilon_{\mathrm{r}}(\omega) = \epsilon_{\mathrm{r}}'(\omega) - \mathrm{j}\epsilon_{\mathrm{r}}''(\omega) = \left(1+\chi'(\omega)\right) - \mathrm{j}\chi''(\omega) \tag{7}$$

is the relative complex permittivity describing the material. This gives the total current in the frequency domain

$$\boldsymbol{J}(\omega) = \left[\sigma_{\mathrm{DC}}\boldsymbol{E}(\omega) + \mathrm{j}\omega\boldsymbol{D}(\omega)\right] \tag{8}$$

where $\boldsymbol{D}(\omega) = \epsilon_0\epsilon_{\mathrm{r}}(\omega)\boldsymbol{E}(\omega)$. In the measurements, the DC-contribution can not be separated from dielectric loss, and the measured current will be

$$\boldsymbol{J}(\omega) = \mathrm{j}\omega\epsilon_0\tilde{\epsilon}_{\mathrm{r}}\boldsymbol{E}(\omega) \tag{9}$$

where $\tilde{\epsilon}_{\mathrm{r}} = \epsilon_{\mathrm{r}}'(\omega) - \mathrm{j}\left[\epsilon_{\mathrm{r}}''(\omega) + \frac{\sigma_{\mathrm{DC}}}{\epsilon_0\omega}\right]$ is the complex relative dielectric permittivity.

2.2 Metal-semiconductor contact

This section describes the physical conditions at contact between materials, e.g. metallic electrodes and powder sample, and is mostly based on [2]. The presented theory is relevant for the present analysis since SiC is known to demonstrate electric properties similar to those of semiconducting materials.

2.2.1 Schottky barrier

Due to the difference in the material properties, the contact between a metal and a semiconductor creates a potential barrier . The semiconductors energy-band must bend to force it to coincide with the Fermi level of the metal. A charge buildup is created in the semiconductor depletion region and consists of uncompensated acceptors (p-type) or donors (n-type). The metal surface gets an opposite charge to balance this, which can be compared to a depletion region of a p-n junction, and causes the energy-band of the semiconductor to bend. On the surface of a semiconductor there is also usually a thin insulating oxide layer 10-20 Å thick, called an interfacial layer. This layer is however so thin that electrons can still easily tunnel through it and it has only a limited effect on the magnitude of the current.

With no interfacial layer the charge of the metal Q_{m} and the charge of the depletion region Q_{d} must be equal and opposite since the system strives to become electrically neutral. If an interface accumulates a charge Q_{ss} the balance is changed and can be described by

$$Q_{\mathrm{m}} + Q_{\mathrm{d}} + Q_{\mathrm{ss}} = 0 \tag{10}$$

The charge Q_{ss} is then balanced by an increase or decrease of the existing charges. The barrier height will be determined by the sign of the charges and an increased metal charge influence raises the barrier and it is lowered if influenced by the semiconductor.

2.2.2 Conduction mechanisms

There are four ways for electrons to be transported through the junction under forward bias. This section contains brief explanations of these conduction mechanisms to give an insight on the reasons behind the measured current. The current is transported by a combination of the following and illustrated in Figure 2:

- Emission over the barrier
- Tunneling through the barrier
- Recombination in the depletion region
- Hole injection (recombination in the neutral region)

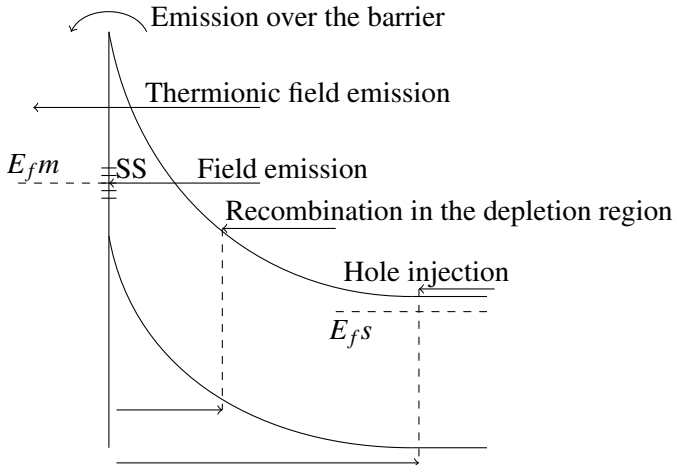

Figure 2: Emission over and tunneling through a Schottky barrier.

2.2.3 Emission over the barrier

To be emitted over the barrier electrons are transported through the depletion region by diffusion and drift in the electric field to arrive at the interfacial layer as

$$\boldsymbol{J} = qn\mu\boldsymbol{E} + qD_{\mathrm{n}}\frac{\mathrm{d}\,n}{\mathrm{d}\,x} \tag{11}$$

where q is the electron charge, n the concentration of electrons (n-type), μ the mobility, $\boldsymbol{E}$ the electric field and D_{n} is the diffusion constant. At the interface emission is determined by the rate electrons transfer across the boundary. This can be seen as a series connected process. If

there is a surplus of electrons at the interface to support the maximum rate of electron transfer that is the limiting factor. If that is not the case diffusion and drift is the limiting factor. This is the main contribution at low electric fields.

2.2.4 Tunneling through the barrier

In heavily doped semiconductors at low temperature, a current is initiated from the tunneling of electrons with energies close to the semiconductors Fermi energy and this is called field emission. With increased temperature, electrons are excited to higher energies and this makes the tunneling probability increase rapidly since the barrier becomes thinner at higher energy levels. However, the number of electrons that achieve the higher energy decreases rapidly further up and a maximum contribution to the current is reached and is known as thermionic-field emission. If the temperature is increased even further and all electrons have enough energy to go over the top, the effect of tunneling becomes negligible and pure thermionic emission is achieved. This becomes more relevant as the electric field strength increases.

2.2.5 Recombination in the depletion region

Recombination appears when electron-hole pairs in the system are not in equilibrium. This takes normally place via localized states with energies near the center of the depletion region. A surplus of electrons then recombine with holes in the valence band. Recombination is more likely to be present at low forward bias voltage and when a high barrier is present.

2.2.6 Hole injection

If the height of the barrier (n-type) is more than half of the depletion region, the region of the semiconductor closest to the metal becomes p-type and thereby contains a surplus of holes. The holes might then diffuse into the neutral region and recombine with electrons from the conduction band.

2.3 Model of SiC

2.3.1 Particle contacts

SiC powder consists of small grains with diameters in the micrometer range. Each grain can be thought of as a sphere for simplification, but in reality the grains differ in shape. If assumed to be spherical, a grain-to-grain contact would appear as in Figure 3.

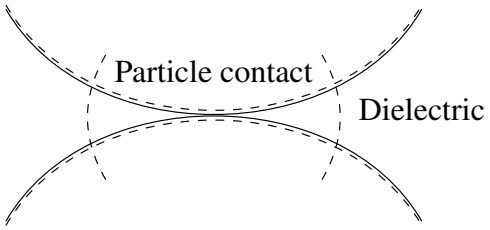

Figure 3: A model of a spherical grain-to-grain contact with a thin surface layer and dielectric capacitances illustrated.

According to [3], a contact between grains can be characterized by a nonlinear resistance, R_s, and a nonlinear capacitance, C_s, between the grains, represented as a reverse-biased Schottky-like barrier. There is also a capacitive contribution, C_d, in the surrounding dielectric depending on the shape of the grain. An electrical model of a single grain contact is shown in Figure 4.

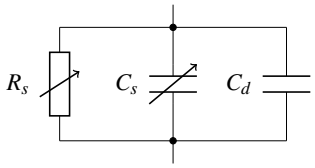

Figure 4: A circuit model of a single grain contact, several in series creates a whole grain column.

Due to difficulties of measuring a single grain a larger sample is used. The complete model of a sample then consists of several grain columns with several grain-to-grain contacts, this is illustrated in Figure 5.

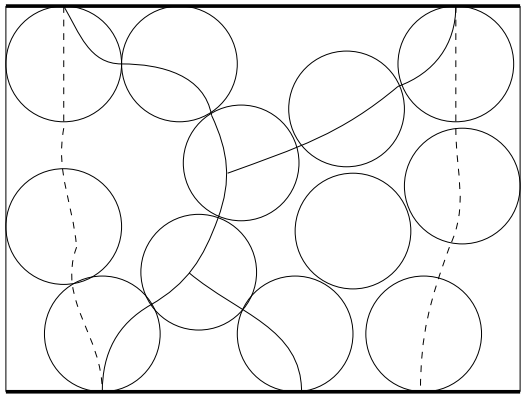

Figure 5: A model of a sample with grain columns and rows, illustrated with resistive (lines) and capacitive paths (dashed).

At every grain-to-grain contact a Schottky-like barrier will arise and it will accumulate charge at the semiconductors oxide layers. This is due to impurities in both the semiconductor surface and in the oxide layer, resulting in dangling bonds which traps impurity atoms. As stated in Section 2.2 the barrier height is determined by the difference in material properties and charges. Even with little difference in the material properties of two SiC grains their oxide layer accumulate charge and the barrier is mainly influenced by these. When voltage is applied one side is forward- and the other is reverse-biased. In Figure 6 a n-type grain-to-grain contact is illustrated, the charge is positive and will bend the semiconductors bands downward. The reversed biased grain bands will bend more due to its depletion region give a higher contribution to the positive charge.

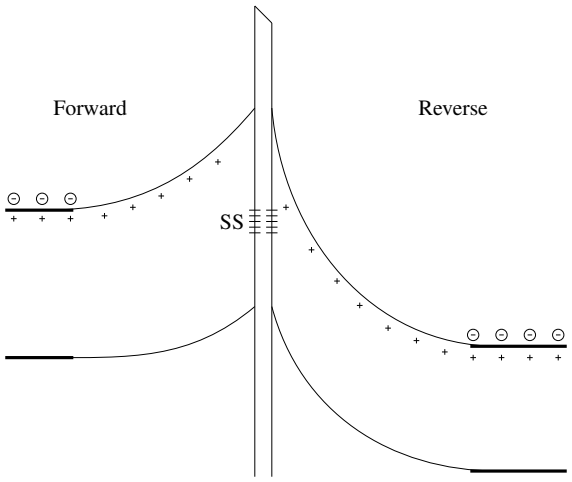

Figure 6: A Schottky barrier between two grains with surface states (SS) at the barrier.

3 Method

There is no existing standard for measuring the conductivity of SiC powder. This led to the adaptation of an experimental approach throughout the project. A measurement cell that in the past has been used for measurements of both breakdown voltages in solid dielectrics and for conductivity measurements of powders was used as a starting point. In particular it was utilized to detect key variables by conducting a multitude of measurements, keeping track of known and suspected variations and their influence on the result. The work proceeded by implementing hardware solutions and changes in the measurement execution that was theorized to curb the variances and stabilize the result.

In general, a measurement consists of two components, a measurement error and a true value. The measurement error consists of unpredictable faults such as noise from outside disturbances or from the measurement equipment itself. These are called stochastic faults or type A faults and results in fast variations in measurements. The true value can differ due to changes that affects the sample, for example variations in temperature, pressure or time. This is called systematic faults or type B faults and gives large and/or slow variations to measurements.

Type A measurement errors can be minimized by removing outside disturbances by shielding the measuring equipment. But they may also arise from the inherent measurement uncertainty of the measuring equipment if the magnitude of the quantity is close to its lower operation range. This can be avoided by making sure the sensitivity of the measurement equipment is well below the measured value.

If the true value of a quantity to be determined is unknown, an elimination process of contributing type B faults can be conducted to investigate their influence on the measurement. This can be done by initializing all known and controllable variables to a constant value. By then introducing a controlled variance in one variable its impact can be determined. Its influence can then be compensated either numerically or by fixating the variable and standardize further measurements to a certain set value.

The main pieces of measurement equipment that was utilized consisted of an insulating diagnostic system called IDA200 that was used for AC measurements and an Agilent 4339B, a high resistance meter with an on-board voltage source that was used for DC-measurements. These supply enough accuracy that type A faults can be neglected.

Type B faults affecting the results are what this project has focused on and attempted to minimize.

The absolute value of the conductivity of the material is not of interest in this work. Since it is a powder, even considering an absolute value might be hazardous since it is deemed to change if the arrangement of the individual SiC particles change within the considered volume. Instead, the work has aimed to produce a methodology that returns the conductivity for an arbitrary amount of SiC powder for which conductivity can be assumed to be uniform, with as little variation as possible between subsequent measurements. The difference between repeated measurements is used to quantify the repeatability of different methodologies.

3.1 Conductivity measurements

There are several ways to measure conductivity. In general, they result in conductivity values within a certain range and provide different information. Three methods have been considered which have their advantages and disadvantages, but each can be utilized to compare the conductivity of different samples. The following methods of measurement was used

- Time dependent DC measurement
- Dielectric response measurement (AC)
- DC-extended measurement

Each method returns a resistance from which the conductivity can be calculated using

$$\sigma = \frac{RA}{h} \tag{12}$$

where R is the resistance, A the area and h the height of the sample.

3.1.1 Time dependent DC measurement

This method consists of applying a DC-voltage and measuring the current passing through the sample. As described in section 2.1.1, the true value of the conductivity can only be found when $t \to \infty$. However, when a comparison between samples is of interest the time can be limited. If the material responds like a dielectric, superposition of the polarizing and relaxation currents can be used to find the conductivity.

3.1.2 Dielectric response measurement (AC)

This method is used to analyze how the material reacts to one or more frequencies of sinusoidal AC. By studying the dielectric loss in the material an electric model of the system can be made. As stated in section 2.1.2, the effective relative permittivity $\tilde{\epsilon}_\mathrm{r}$ is measured and transformed into a complex capacitance with area and sample height as

$$\tilde{C} = \frac{A}{d}\tilde{\epsilon}_\mathrm{r}. \tag{13}$$

A current through the material consists of a resistive part, resulting in losses, and a capacitive part as illustrated in Figure 7 a). The figure is an example of a parallel plate capacitor with a loss angle which can be described by its complex capacitance also shown in Figure 7 b).

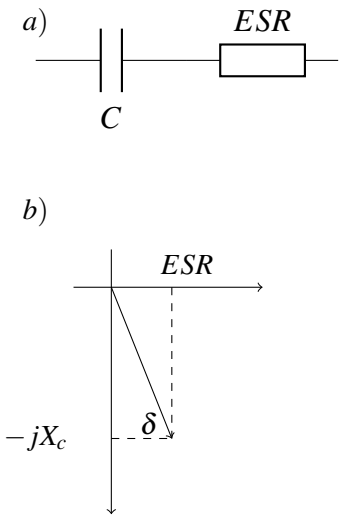

Figure 7: A representation of a parallel plate capacitor with losses. a) is a circuit representation with an ideal capacitor and a equivalent series resistance. In b) the loss angle δ is shown.

The insulation diagnostic system returns C' and C'' over a range of frequencies from which the impedance of the measured sample can be found by

$$\tilde{C} = C' - jC'' = \frac{1}{\mathrm{j}\omega Z} \tag{14}$$

where $Z = R + \mathrm{j}X$.

As stated in Section 2.3.1, SiC can be modelled by a resistance in parallel with two parallel capacitances. An ideal response with a resistance in parallel with a capacitor is seen in Figure 8. However, since the SiC model has elements which are nonlinear, the response might differ from the ideal case.

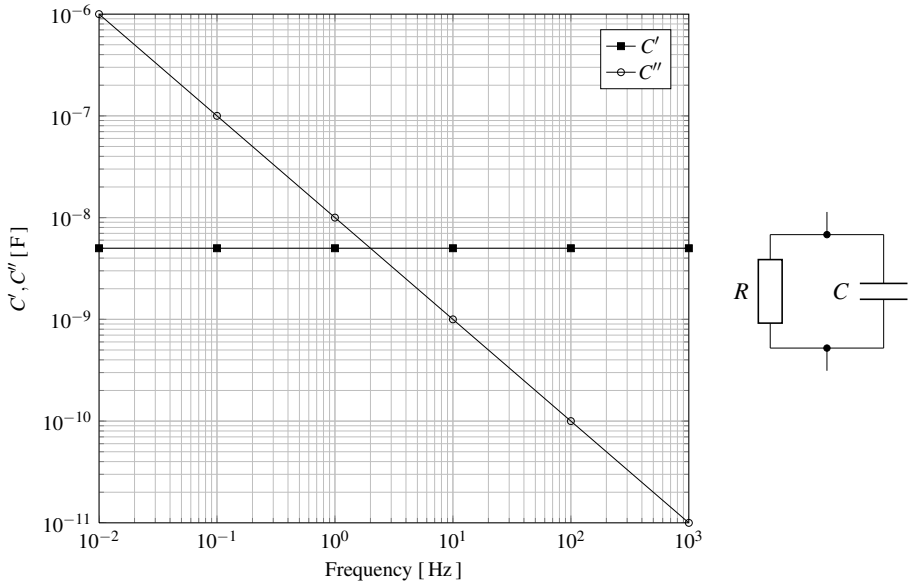

Figure 8: An example of a dielectric response of an resistance and capacitor in parallel.

AC measurements can also be interpreted by using another model of the material [4]. By plotting the response of the complex impedance $Z(\omega) = Z' - jZ''$, the bulk and barrier contributions to the measured impedance can be separated, as illustrated in Figure 9. This enables another interpretation of the material properties.

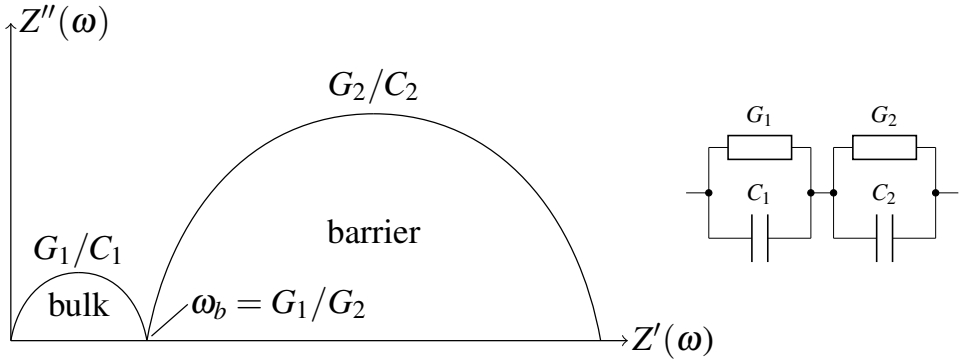

Figure 9: An illustration of the bulk and barrier interpretation of the material and how it relates to the impedance.

3.1.3 DC-extended measurement

This method can be used to study the nonlinearity of the material. By applying an increasing DC-voltage in steps the conductivity in a wide range of electric fields can be measured. There are several ways of doing this. Preferably, a system that produces conductivity results with a high repeatability is used and a new sample is used for each voltage level. A more practical way of conducting this type of measurement is to subject the same sample to an increasing voltage and record the current, but this does not produce a true voltage-current characteristic of the linearity as the material will polarize with time.

3.2 Initial attempt

A powder measurement cell as seen in Figures 10 and 11 was used to conduct an initial study of the different measurement techniques and to quantify the accuracy and repeatability of the measurements. The measurement cell is made of stainless steel and implements a guarded three-electrode system, seen in Figure 12.

An amount of sample of roughly 5 mL was collected and inserted into the cell using a funnel. The sample surface was flattened by softly hitting the cell with a rubber hammer. The screw cap was then mounted on top. The screw was rotated with an amount of degrees, equal every time, compressing the spring and applying pressure to the sample. Since the tightening screw was never removed from its thread, this was the best way available of applying force with the same magnitude each measurement. The equipment was then connected to the cell and the measurement conducted. After the measurement the cell was disassembled. There was sufficient friction between the plastic insulating cylinder and the electrode that it remained in roughly the same position as during the measurement. This enabled an, albeit noisy, measurement of the sample height. It was also possible to measure the height of the sample itself when the cell was disassembled. In Figures 13a-13d the results from the initial measurements are presented.

Figure 10: The measurement cell.

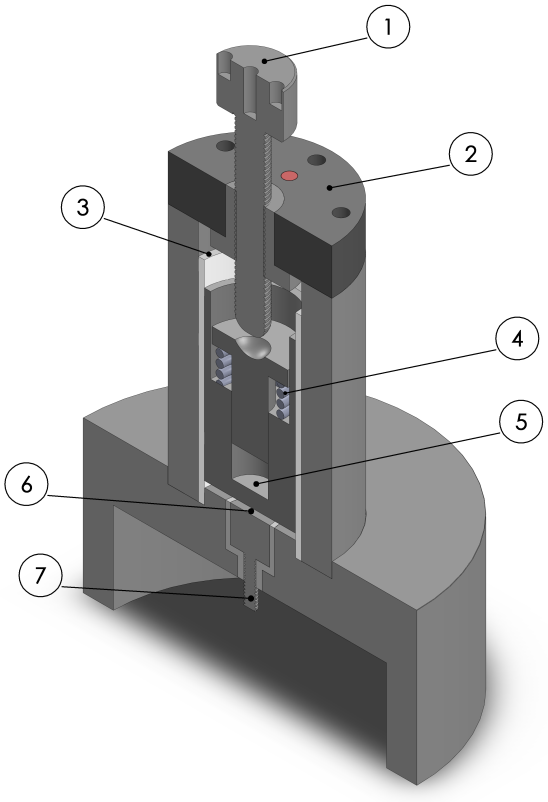

Figure 11: A section view of the measurement cell. 1. tightening screw, 2. top cover, 3. insulating plastic cylinder, 4. spring, 5. electrode, 6. sample space, 7. output.

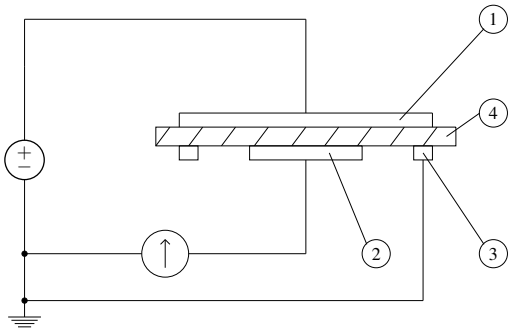

Figure 12: A guarded electrode system for volume conductivity measurements, 1. upper electrode, 2. measuring electrode, 3. ground electrode, 4. measured sample.

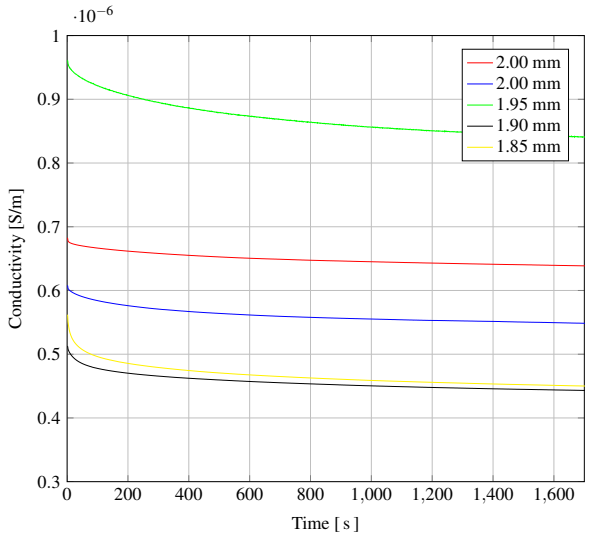

(a) DC-measurements

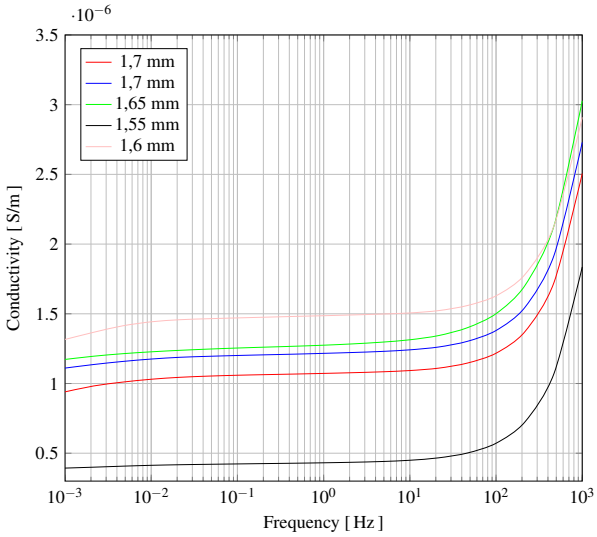

(b) AC-measurements

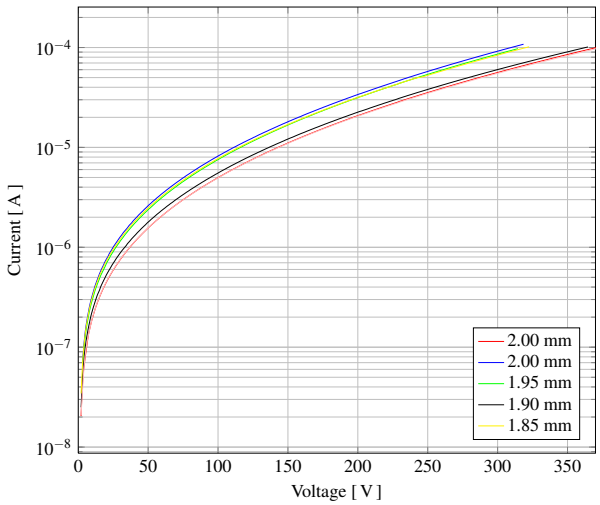

(c) DC-extended

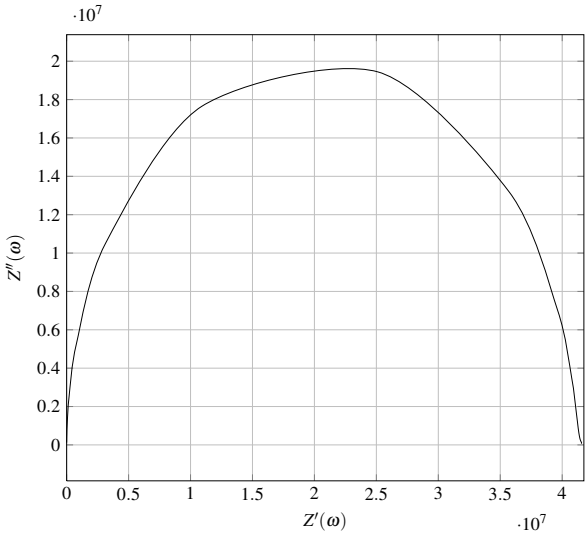

(d) Bulk and barrier

Figure 13: Initial DC and AC measurements.

3.2.1 Observations

As seen in Figure 13 the initial measurements had a relatively large spread and none of the different ways of measuring produced results with satisfactory repeatability. A large variation between samples was seen within each measurement type, even with seemingly similar measurement conditions. However the results gave an insight into the different measuring methods and improvements needed to enhance the repeatability.

The AC, DC and DC-extended measurements all display large deviations between the lowest and the highest recorded values, between two to three times. Further series were conducted and it seemed that the repeatability between these types of measurements are the same, the difference between them is the information they yield.

Various sample heights were tried by varying the amount of powder in multiples of 5 mL. These series indicated that increasing the amount of powder made the repeatability worse. Decreasing the amount further was considered impractical. Measuring with a sample height between 1 and 2 mm was also practical since enabled limited comparisons with existing research.

As opposed to a linear material, changes in conductivity could be present even with small variations in the height of the measured powder. But the results show that with increasing sample height the measured conductivity does not always decrease. The height of the samples was measured by disassembling the cell after being energized and measuring the height of the sample using a caliper. This procedure may have lead to uncertainties which influenced the obtained conductivity values. The results of the measurements could also depend on other factors such as the force applied not being equal across the measurements.

The bulk and barrier method, Figure 13d, produces one of the semicircles that was expected, but the frequency window of 1 mHz to 1 kHz may be too narrow to resolve both the bulk and the barrier.

While the method of measuring the amount of powder in a sample at this time was known to be inaccurate, its contribution to the error was deemed too small to account for the large variations in the measured conductivity values.

3.2.2 Polarization

During the measurements a continuously decaying current was observed, which was expected due to polarization in the material. This was further studied with long time measurements and an example is seen in Figure 14. The current decreased rapidly in the beginning but seemed to stabilize after a while, the time this took did vary between measurements.

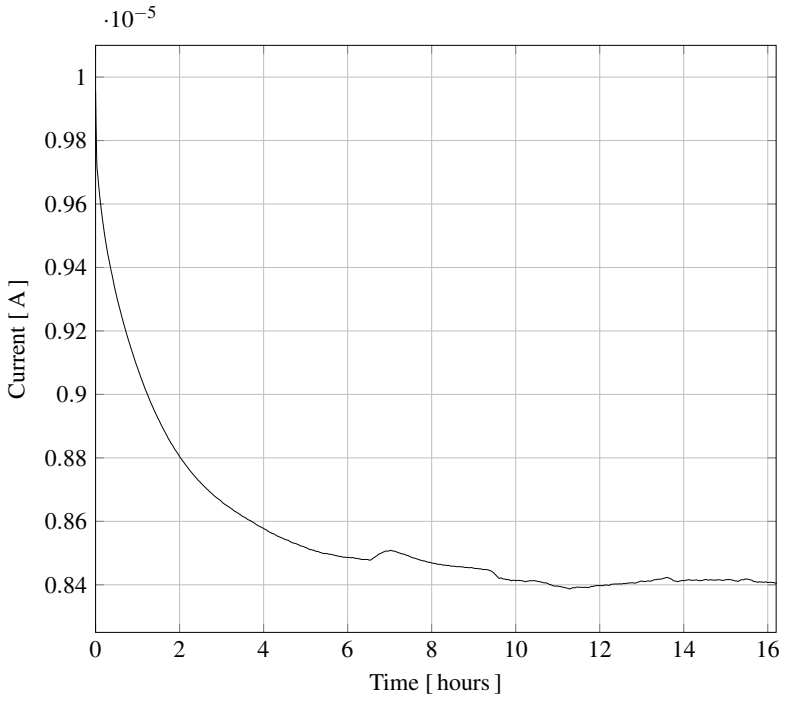

Figure 14: A 16 hour measurement that shows a steady decrease in the current over time but with noise in the later parts.

Figure 15 shows the response when the voltage was set to zero after 30 minutes of energizing and relaxation begins. In section 2.1.1, the concept of superposition was introduced. That requires the relaxation current to be of the same magnitude as the polarization current, which it is not. SiC is a semiconductor and does not exhibit a dielectric response. Thus, superposition can not be used to find the value of the conduction current.

Relaxation was further investigated by two measurements, the first comprised of letting the cell rest with the electrode connected in different ways. The measured currents are shown in Figure 16. In the experiments the voltage was turned off after ten minutes and the dotted lines indicate the time that the voltage was off. After an hour the voltage was turned on again and the recorded currents appeared to be dependent upon conditions of the test cell between the measurements. The effect of switching the test voltage on and off during long time measurements on the recorded current is shown in Figure 16.

The expected result of these two measurement was to find an equal or, due to relaxation, higher current when the voltage was turned back on. Instead, the opposite was found. There appeared to be either ongoing polarization even when the voltage was turned off, which was considered unlikely, or a change in the measurement conditions causing the lower current.

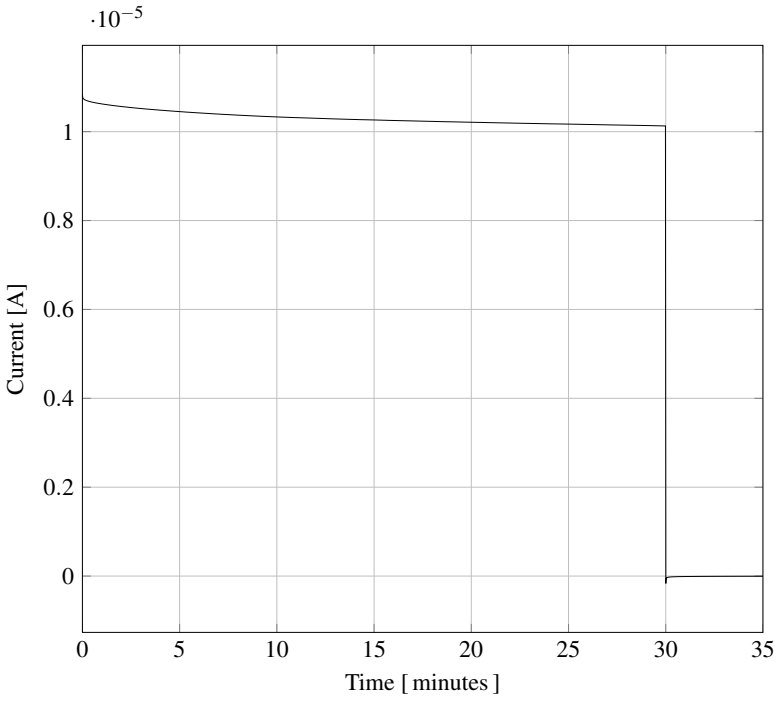

Figure 15: Polarization and relaxation.

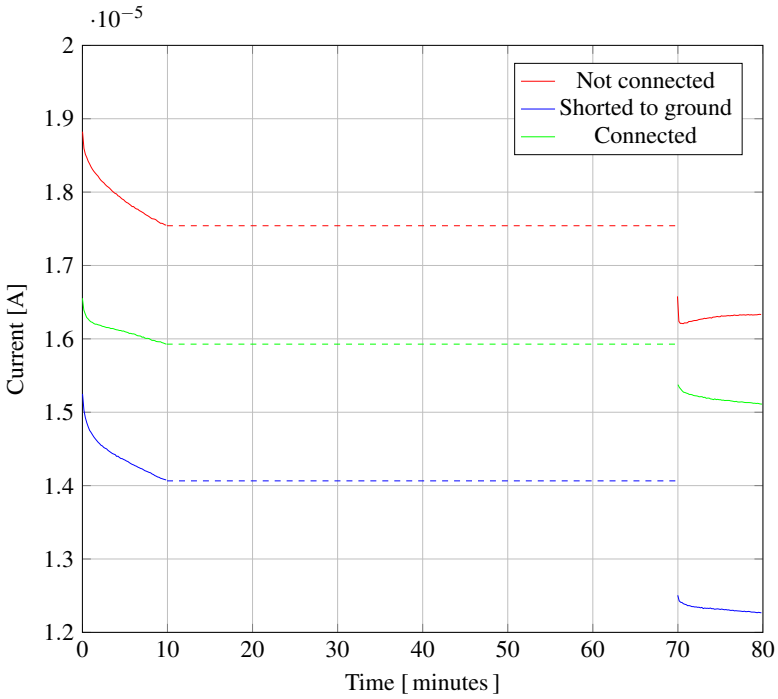

Figure 16: Relaxation given three different electrode connections.

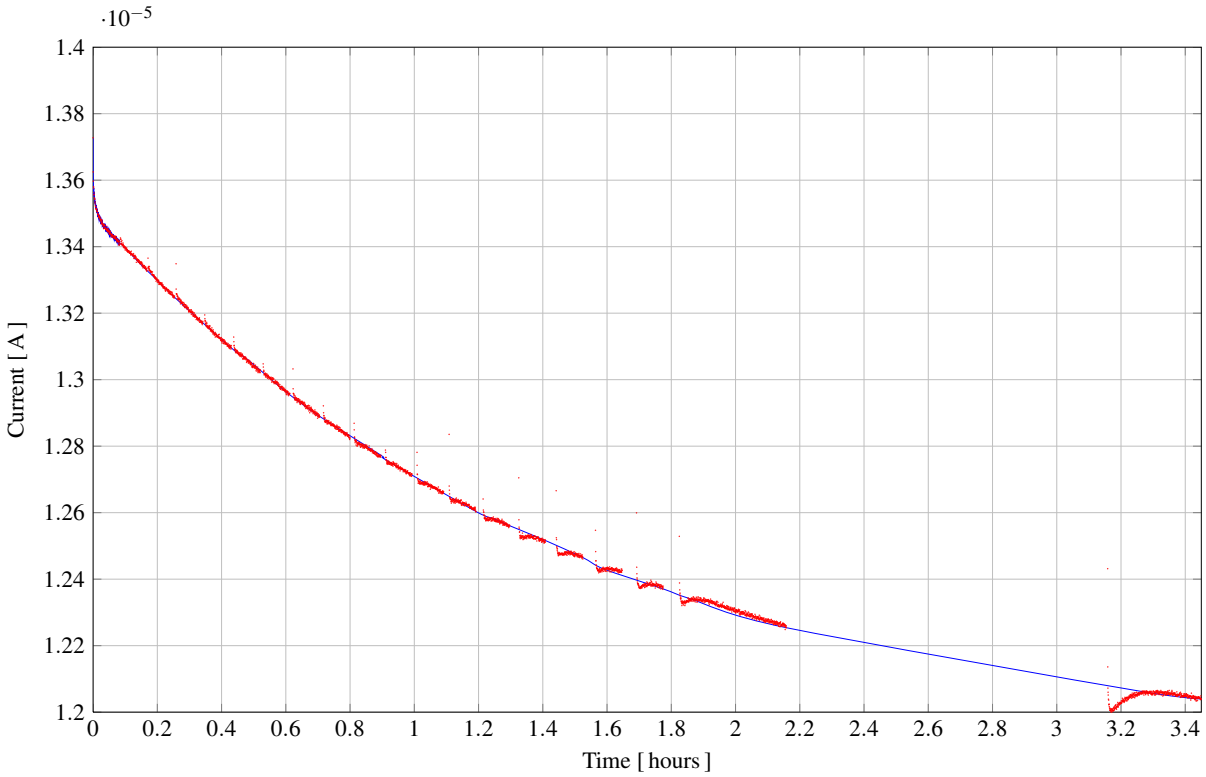

Figure 17: Behavior when voltage is turned on and off with increasing time.

3.2.3 Cell problematics

From the results of the experiments with the original test cell, the reasons for the large deviations of the measured data were identified. It was observed that the spring inside the electrode system presented a problem. Firstly, it prevented measuring the sample height when the cell was assembled and the powder was under pressure and secondly, the torque applied to the screw did not directly translate into a clamping force acting on the sample as there is:

- Friction between the thread and tightening screw, depending on dust in the thread, thread wear and lubricant
- Friction between the contact areas of the electrode and tightening screw
- Friction between the electrode and the plastic insulator

Due to these reasons, it is not possible to apply an amount of torque and get a proportionate force repeatedly.

Another issue is the fact that all of the above stated friction contributions change with time and usage. The thread becomes increasingly worn, the spring characteristic change, the lubricant differs etc. If the cell is to be prepared with a given torque and the original electrode is used, the measured values will differ with time.

A set of improvements to the measurement setup are presented in the next section.

3.3 Improvement attempt I

It was suspected that the material properties were temperature and pressure dependent and that even small variations in these variables causes a large change in the conductivity. With the original cell the only variable that was under complete control was the length of the measurement. The design goals of the modification was to enable an accurate measurement of the clamping force as seen by the sample, to record the temperature during the measurement and to provide a way to measure the sample height externally while the sample was in the cell and under pressure. The aim was to achieve a better repeatability and to quantify how small variations in the input variables affect the conductivity.

To measure the clamping force applied to the sample a load cell was built into the electrode. Figure 18 shows the planned modification. By removing the spring from inside the electrode it enabled the measurement of the sample height from outside the cell. Two pieces of plastic holds and insulated the load cell. An aluminum spacer separated the top cover from the upper guard cylinder slightly, allowing the cable from the load cell to pass out. The cable itself was isolated using heat shrinkable tubing.

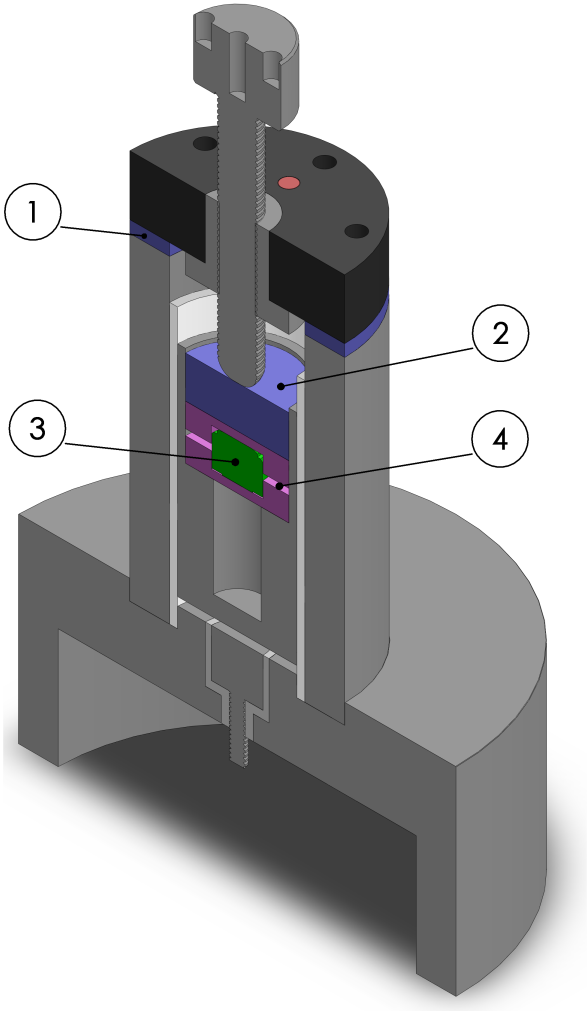

Figure 18: The planned modification of the measurement cell, 1. aluminum spacer, 2. aluminum contact slug, 3. load cell, 4. plastic insulators.

To measure the temperature of the cell an 8 mm thick solid aluminum disc was made with a NTC-thermistor fitted inside using epoxy mixed with thermal compound. The disc was placed on a table and the cell was placed upon the disc. Another thermistor of the same type was suspended in the surrounding air and used to measure the ambient temperature and the thermal inertia of the system.

It is apparent that it was not the actual temperature of the sample that is measured. The obtained temperature value was made up of contributions from the bottom of the cell, the table that the disc rests on and ambient air temperature. This might seem inadequate but the goal was to determine whether changes in temperature correlates with changes in conductivity, for which this way of measuring was adequate.

Data acquisition was realized by a measurement circuit board, Figure 19, where four signals was measured: cell and ambient temperature, load cell output and the supply voltage. The latter was needed since the outputs of the three former was dependent on the supply voltage. The signals was quantified by a 16-bit ADC operated with a single supply yielding 15 bits of resolution.

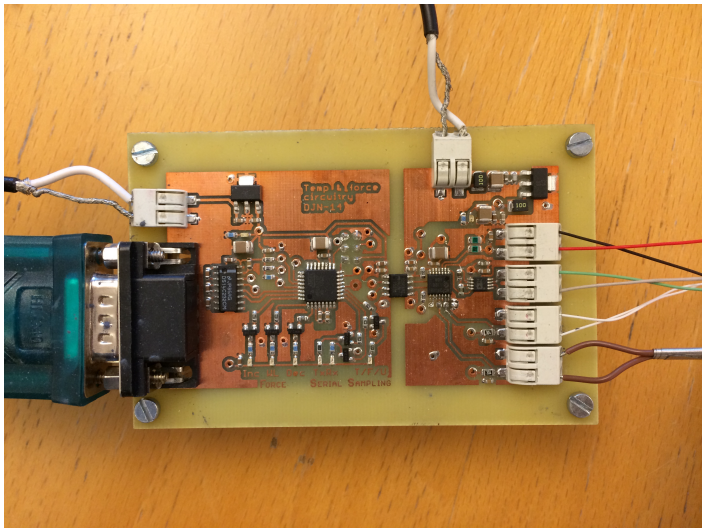

Figure 19: The acquisition electronics.

The load cell is essentially four strain gages connected as a bridge enclosed in a stainless steel container. The output is differential and nominally 1.5 mV/V. The signal is conditioned by a differential instrument amplifier with a gain of 200 before being sampled by the ADC. The gain is set by the quotient of two resistors from the same series; the gain is stable even with temperature variations in the substrate and surrounding air.

The thermistor form an unknown resistance in a voltage divider and the temperature was found by calculating the resistance of the thermistor. This was possible since the other resistance, the supply voltage and the output voltage from the voltage divider was known. A third degree Steinhart-Boltzman equation was used to calculate the temperature from the resistance of the thermistor.

The PCB was split in two parts, one analog and one digital part, each with a separate galvanically isolated supply. The digital side housed an Atmel microcontroller that communicates

with the ADC-chip over an I2C-bus through a chip that galvanically isolated the signals using transformers. The microcontroller serially transmitted data to the measurement computer via a RS232 level shifter. The original software that was used to communicate with the resistance meter was extended to allow for the necessary conversion and logging of the measured data into the same file as the measured current. The analog side of the board featured a more heavily filtered linear regulator than the digital side, providing the sensors with a relatively stable supply voltage where switching spikes and noise from the AC-DC converter was heavily suppressed. Care was taken when routing the analog side to avoid ground loops and bad return paths. It was star grounded and star fed. Instead of ordering the PCB, it was decided to manufacture it at a local lab to lower the costs and to speed up delivery. A schematic of the acquisition board can be found in Appendix A as well as the circuit board layout.

Figure 20 shows the modified cell along with the acquisition board. Figure 21 shows the new way of measuring sample height.

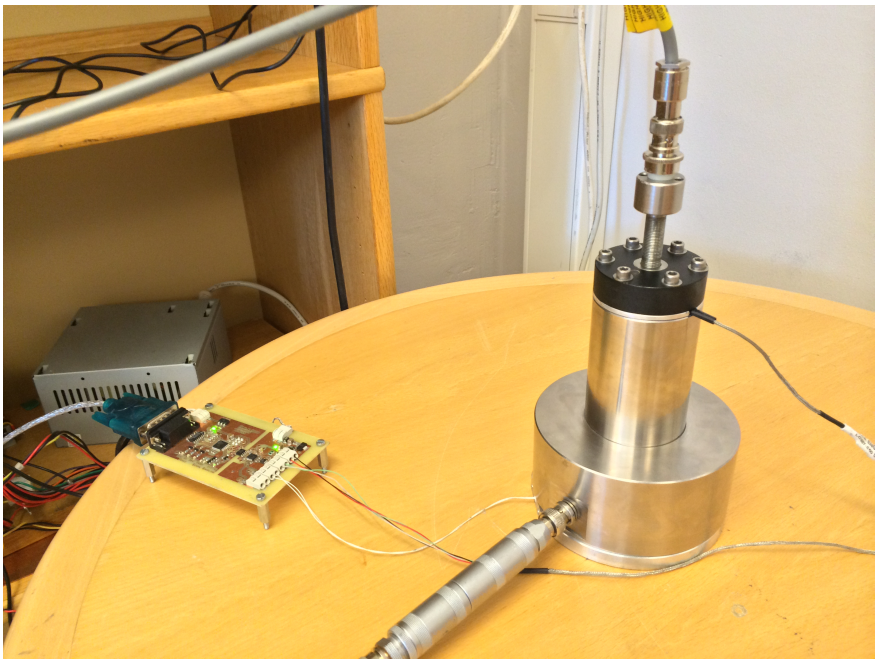

Figure 20: Measurement setup

Figure 21: The sample height was measured using an adjustable parallel and a micrometer.

3.3.1 Evaluation

It was immediately clear that the modifications had not yielded the anticipated result. The measured force was found to be exponentially decreasing as seen in Figure 22. It was theorized that the plastic spacers were slowly deforming and causing the decreasing force. To harden their response, it was tried to fill the cavities where the load cell resides with epoxy and turning them again to flatten the surfaces, but that changed nothing. Another attempt was made by manufacturing two steel discs which replaced the epoxy, which resulted in a marginal improvement. The spacers with the steel discs are shown in Figure 23.

By putting the two plastic spacers and the load cell in a vice the exponential decrease in force could be reproduced. If they were removed and the load cell was put in the vice alone the force was constant, indicating that the plastic was deforming and responsible for the decreasing force. However, if the spring was reintroduced together with the plastic spacers, the force kept constant. Logically the plastic spacers were still deforming, but the spring compensated for that. This led to the design of a new measurement setup, described in the next section.

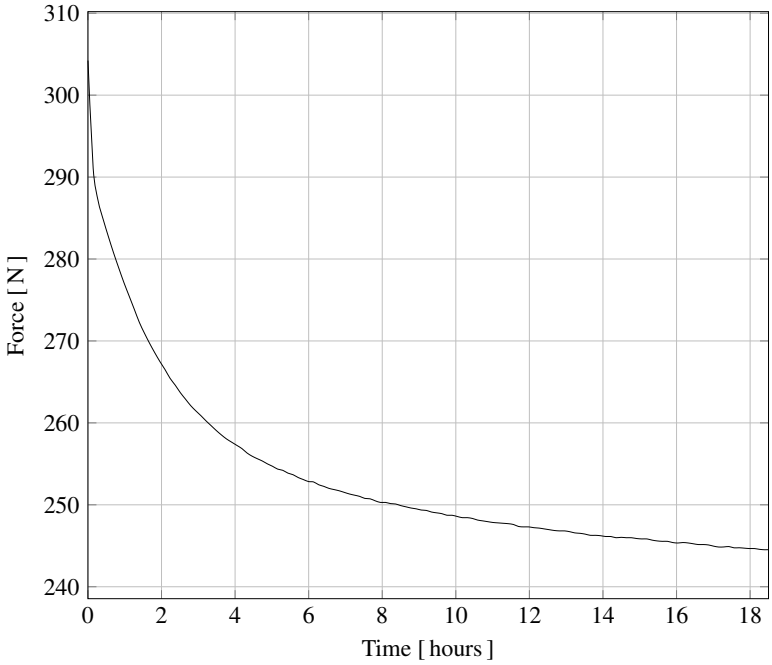

Figure 22: Force applied to the sample

Figure 23: The plastic spacers with the steel discs.

3.4 Improvement attempt II

The realization that the force could be kept constant if the spring was present, even with the plastic insulators, led to the design of a new setup, seen in Figure 24. By reusing the spring and the old electrode as a spring enclosure, force was applied using the original tightening screw held by the original top cover, the latter also insulated the structure. The new electrode housed the load cell and the plastic insulators. All force generated by turning the tightening screw passes through these and and exacts a measurable clamping force on the sample. The new electrode was made in such a way that the adjustable parallels and the micrometer could still be used to measure the height of the sample under pressure. The finished setup is shown in Figure 25.

Unfortunately, not all the problems were solved by introducing these modifications, Figure 26 shows the force with and without the spring present. While this setup improved the situation, the results was far from being acceptable. Another piece that was not taken into account when the experiments with the vice was done was present in this setup. It was the original top cover, which was made of plastic and holds the tightening screw. The spring was not able to compensate for the added deforming material.

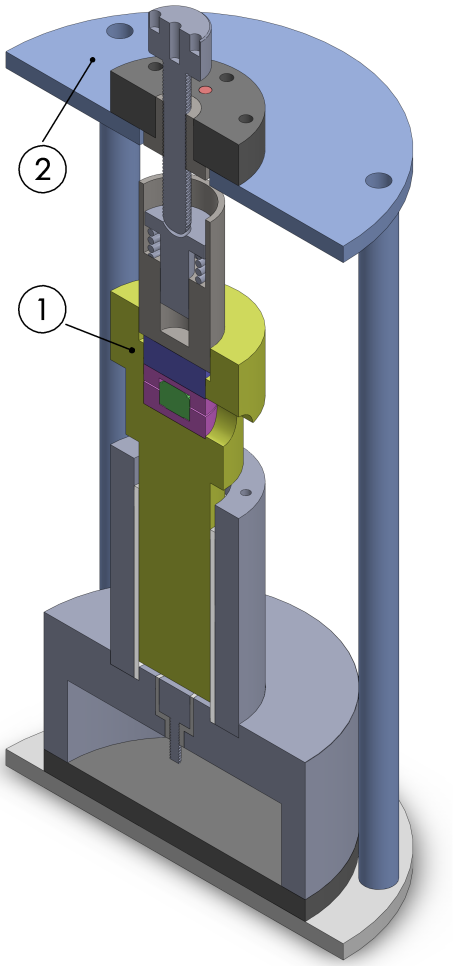

Figure 24: Section view of the new measurement setup, 1. new electrode, 2. support structure.

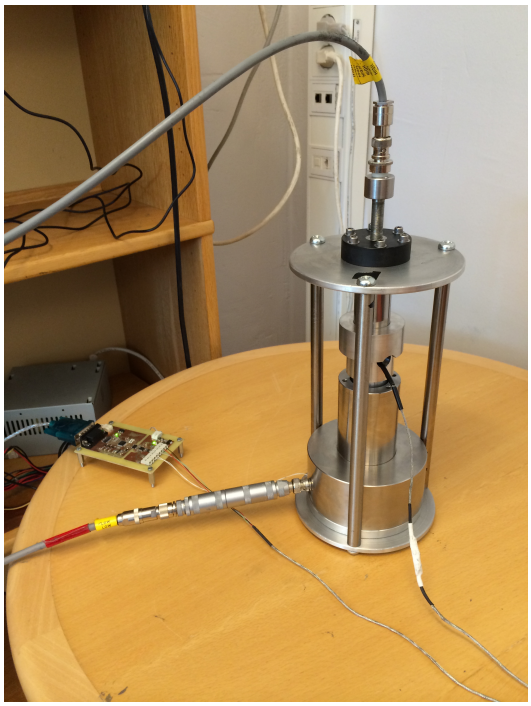

Figure 25: New measurement setup.

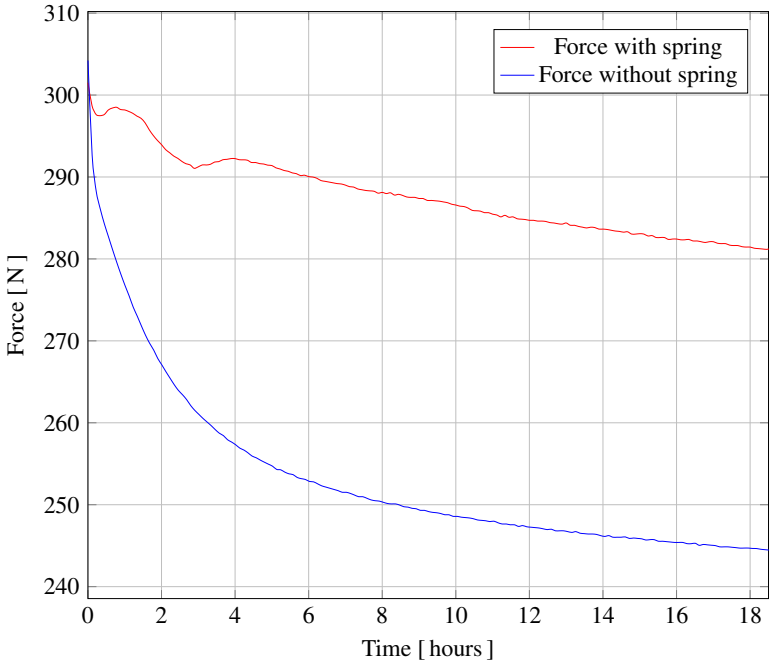

Figure 26: Force comparison between cell with and without the spring. The fluctuations seen on the force with spring curve is most likely due to temperature variations.

To use this setup, it was necessary to apply the force wanted, wait for the force to fall and re-tighten. After a few cycles a ten minute measurement could be done where the force decreased with only a few Newtons. However, it was difficult to reproduce this. The setup did yield some useful information. Figure 27 shows the results of a six day long measurement. It was apparent that the current through the material has a substantial temperature dependence. The current waveform was periodic with a 24-hour period, which correlates with the temperature

waveforms. The observant reader will recall the results of the longtime measurement presented from Figure 14, where the noise in the signal was from temperature variations, but they are of a much smaller magnitude. This is explained by the scheduled operation of ventilation in the room. This work began in the wintertime when the schools ventilation was active, it was later turned off as spring arrived and indoor temperature started fluctuating more, resulting in the larger variations in the current.

The force does not correlate with the current, instead it seemed to follow the temperature with a positive temperature coefficient. The load cell was supposed to be temperature compensated but it may not have worked properly. Mainly since there was little correlation between the force variations and the current.

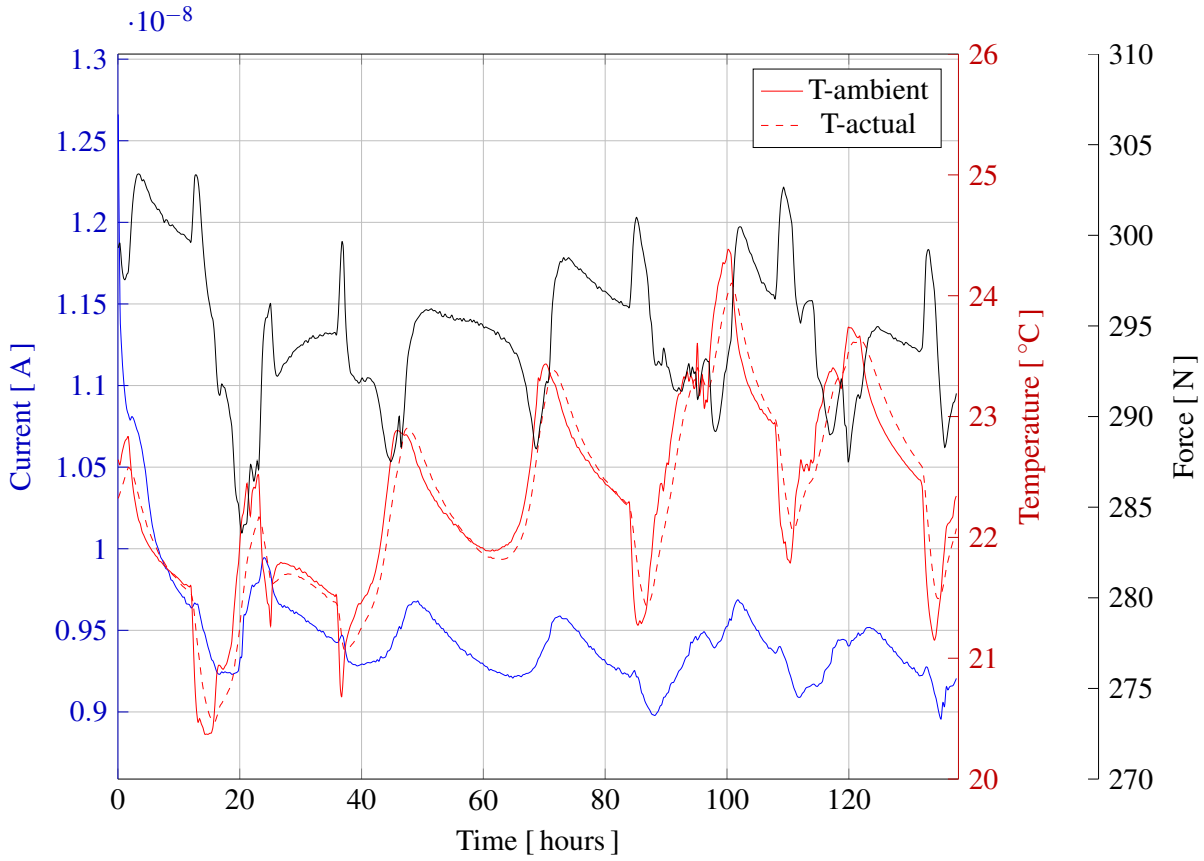

Figure 27: Current, force and ambient and cell temperature over six days.

Due to the large temperature variations and their influence on the current, a plan to achieve a constant cell temperature was devised. It involved heating the bottom plate electrically by regulating the power dissipated by resistors via PWM where the duty cycle was decided by a PID-regulator. The already in place thermistor in the bottom plate was used for feedback.

Manufacturing a new PCB with both the measurement electronics and the power electronics needed for controlling the resistors would have been the best solution in turns of minimizing the complexity of the computer software and the system overall. However, due to cost concerns, a new board was designed that incorporated an Atmega, an RS232 converter, a power MOSFET and some gate driving circuitry. Schematic and board layout are available in Appendix B. Figure 32 shows the manufactured circuit board.

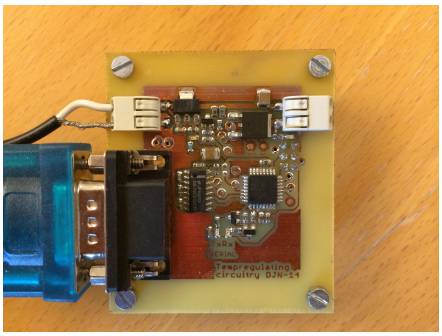

Figure 28: Heating electronics.

The microcontroller runs at 8 MHz, connecting the hardware 16-bit timer directly to the gate driving circuitry yields, without any prescaler, a switching frequency of 122 Hz and resolution of 65536 steps or 0.07 mW per step with a 9 V supply. The maximum power that can be dissipated was 4.6 W.

The actual PID-regulator could have been implemented in either the the measurement computer or in one of the embedded controllers. Having it reside in the computer was proven to be most practical since it allowed for easy adjustment of the regulating parameters. It was therefore merged with the rest of the controlling software. The set point for the temperature controller was chosen arbitrarily to 25 °C, and the results are shown in Figure 29. Note that T-actual is very close to 25 °C and that the current now has a shape that is closer to that one would expect from polarization.

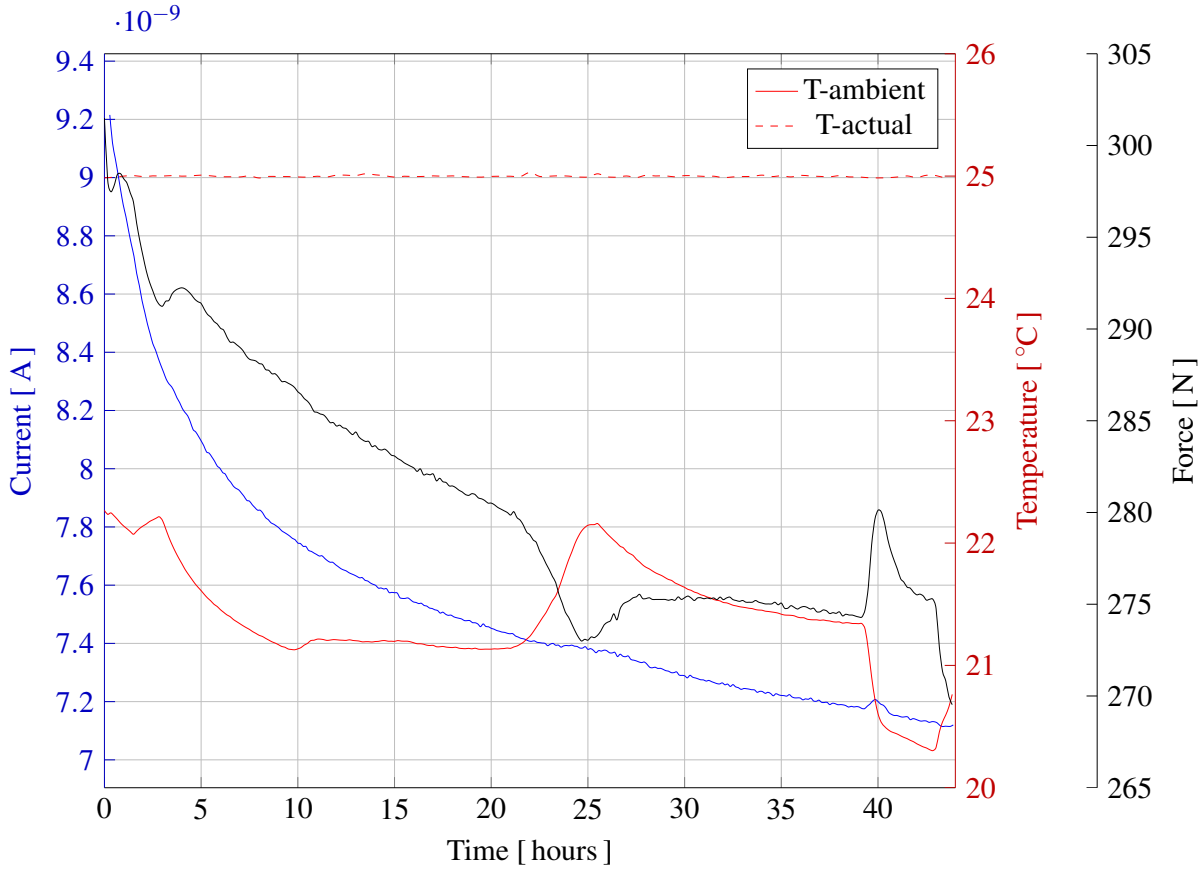

Figure 29: Current, force and ambient and cell temperature over 44 hours.

In the initial measurements, it was noted that even when voltage was not applied to the cell, some form of polarization or change in the variables that influences the current through the material was occurring. Observing how to force behaves both with and without a spring and knowing that the current through the material decreases with decreasing force, it was clear that it was a loss of pressure that caused that phenomena.

Given that the measurement setup was still not able to produce a constant force, a new setup was designed. It is described in the next section.

3.5 Improvement attempt III

A simple and robust way of maintaining constant pressure is to work with a mass in cooperation with Earths gravity. This realization led to the design of a new upper electrode system with enough weight to be able to apply a clamping force to the sample of at least 298 N. This is the force which according to [5] is required to avoid electrostatic forces.

There are two forces that affects such a system in an important way. The force acting straight downwards and on the sample, F_{vertical}, and the force that balances the electrode, $F_{\text{horizontal}}$. Ideally, $F_{\text{horizontal}}$ should be zero and the full weight of the electrode should rest on the sample. In order to keep $F_{\text{horizontal}}$ low it was decided that the new electrode should have rotational symmetry and an as low as possible center of mass.

Ideally a solid piece of stainless steel should have been machined into the new electrode. The use of stainless steel was motivated by the need to keep the electrode contact area from oxidizing over time. Unfortunately acquiring such a workpiece would have been an expensive enterprise. Instead, using materials that was readily available, a doable solution was found that used a stainless steel rod as the actual electrode material and cylindrical weights machined from construction grade steel. The weights rest on a locking ring that was fastened to the rod using a shrink-fit. The inner diameter of the locking ring was machined to approximately 5 µm less than the outer diameter of the electrode, using a gas cutting torch, the locking ring was expanded thermally by heating it until red-hot and the two pieces were mated together.

Earlier measurements showed a non-negligible temperature dependence of the results. Given that the new electrodes thermal mass was relatively large and the fact that it was in direct contact with the sample it was decided that it too, along with the bottom heating plate, should be actively temperature regulated. This was realized by manufacturing an identical circuit board as the one used to control the bottom plate and by placing resistors inside a track that was machined into the locking ring. Another instance of a PID regulator was created in the controlling software. The finalized control system is briefly described in Appendix C. The resistors was arranged in two circular layers and the sign of the current differs in each, canceling out much of the generated magnetic field and inductance, eliminating much of the electromagnetic interference caused by high frequency components in the supplied current. The thermistor originally used to measure the ambient temperature was installed in the new electrode, between the locking ring and the guard cylinder, and was used for feedback.

A drawing of the new setup is shown in Figure 30. In Figure 31 the finished setup is shown. A picture of the heating resistors in the locking ring is shown in Figure 32. Note that the bottom plate from the earlier attempt was reused, utilizing upside down screws and nuts enabled the whole cell to be levelled using a spirit level.

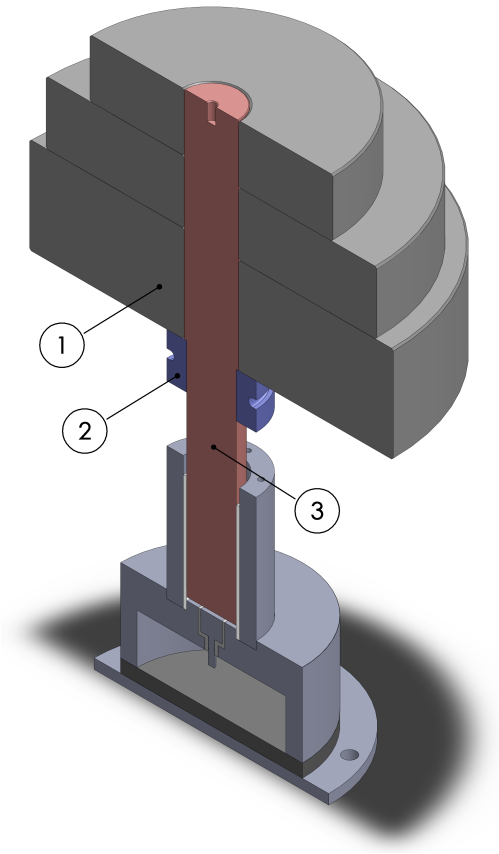

Figure 30: Section view of the new measurement setup, 1. weights, 2. locking ring, 3. electrode.

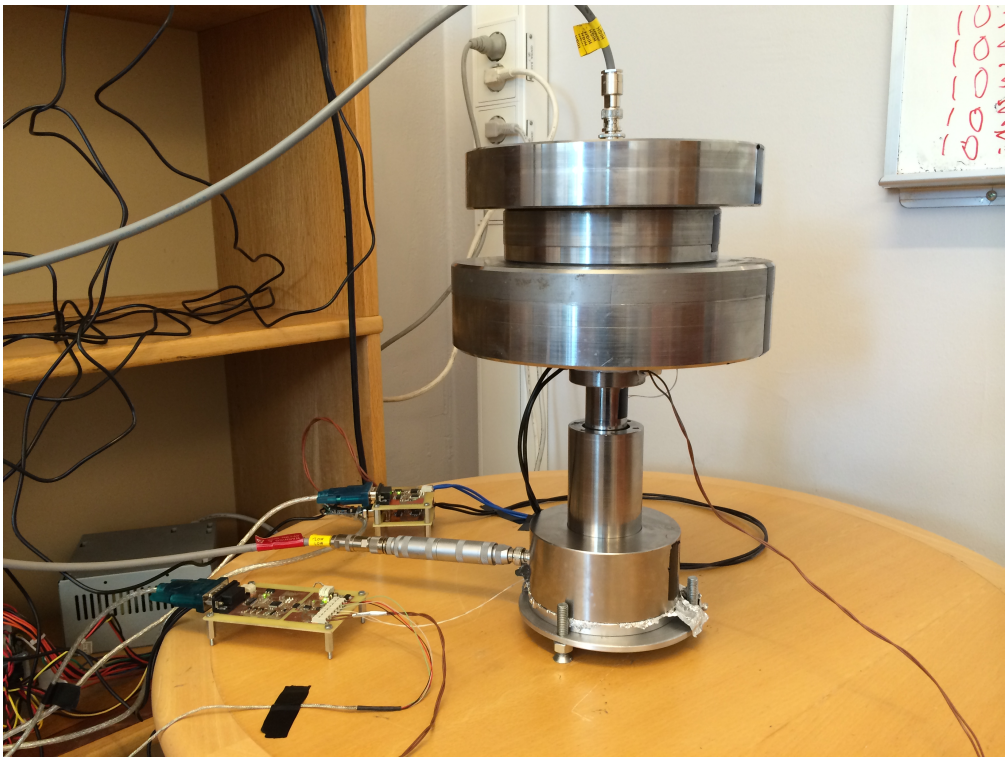

Figure 31: Final measurement setup.

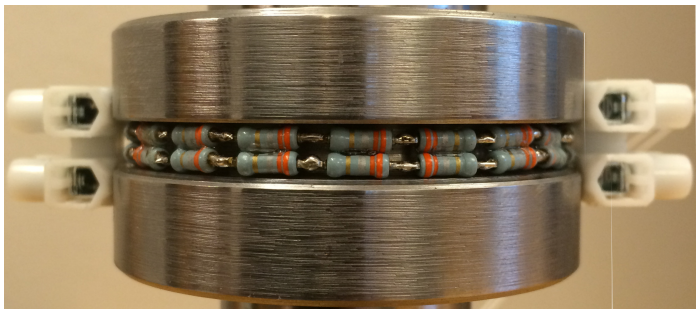

Figure 32: The heating resistors resistors in the locking ring before being covered by epoxy mixed with thermal compound. The terminals blocks visible on either side are the connections for the thermistor and resistors, they also acts as strain relief.

This measurement setup showed promising initial results and it was decided not to manufacture any more hardware, instead focusing on improving the preparation of the measurement and evaluating the results. The final adjustments are described here and the actual results are presented and discussed in the next section.

3.5.1 Finalizing the setup

A large issue affecting the measurements adversely was found to be the insertion of the electrode and application of the weights to the electrode. Originally, after the sample was put inside the cell, the electrode was inserted first and the weights starting from largest to smallest were lowered onto the electrode. It was virtually impossible to apply them without disturbing the electrode and it experienced both horizontal and vertical forces, some of which acted on the powder. This altered its composition and led to large variations in conductivity. The measured conductivity was in the range between what was found with the earlier cell and downwards, sometimes more than a tenth as low.

Several variations were tried, ranging from rearranging the order of which the electrodes were applied to variations in the amount of weights. After some trial and error, a solution was found. Instead of applying the weights after the electrode was inserted into the cell, which had turned out to be unfavorable, the electrode was inserted with the smallest weight already applied. Preferably the entire stack of weights should have been used, but that would have required some sort of pulley. This turned out to be the best solution overall, including previous measurement setups.

The sample preparation process was changed. By using a scale, 2.000 g of powder was collected and inserted into the cell using a funnel. The amount left on the funnel was measured several times and it was repeatedly found to be 0.02 g. The base part of the cell was then softly hit horizontally with a rubber hammer 20 times clockwise, then 20 times counterclockwise. The plastic insulator was then removed from the cell, cleaned, and reinserted, removing any residual powder left from the insertion of the sample. Then the electrode with the weight was inserted.

An issue that was present during the entire work was finally alleviated. If the electrode was inserted too fast, the air that needed to escape the cell would take some of the power with it. This was visually noticeable in the experiments and was resolved by milling the lower electrode in such a way that a small column is created that the air can flow out through. The final setup is shown in Figure 33.

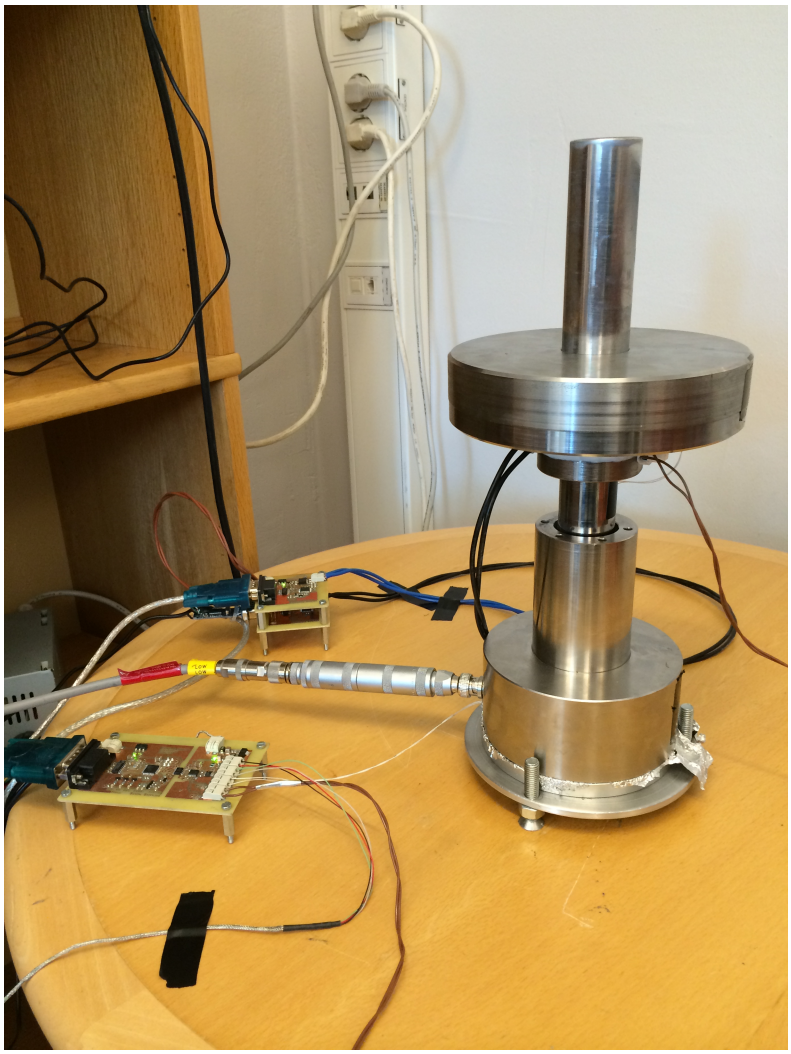

Figure 33: Final setup.

4 Results and discussion

An extended series of experiments consisting of 30, 20 minute, 1 V measurements was conducted aiming at quantifying the repeatability of the system and the process. In Figure 34 the obtained conductivity values are presented.

To evaluate the results both current and conductivity are of interest. One way of measuring the repeatability is to calculate how much larger the highest recorded value is from the lowest recorded value. This is the worst case metric. These values should be as close to a 100 % as possible. Another way consists of calculating an averaged curve out of all the measured data and then computing the deviations from all lines, a sort of mean error, shown in eq 15. The goal for latter is to be as small as possible.

$$\text{average error } = \frac{\sum_{n=1}^{30} |I_{n,20\text{ min}} - I_{n,\text{average, 20 min}}|}{30} \cdot 100\% \tag{15}$$

These two values, calculated using the data recorded after 20 minutes, can be found in Table 1.

Table 1: Results of the final measurement series.

	Current [%]	Conductivity [%]
Largest/smallest	126.4	132.0
Average error	4.7	6.5

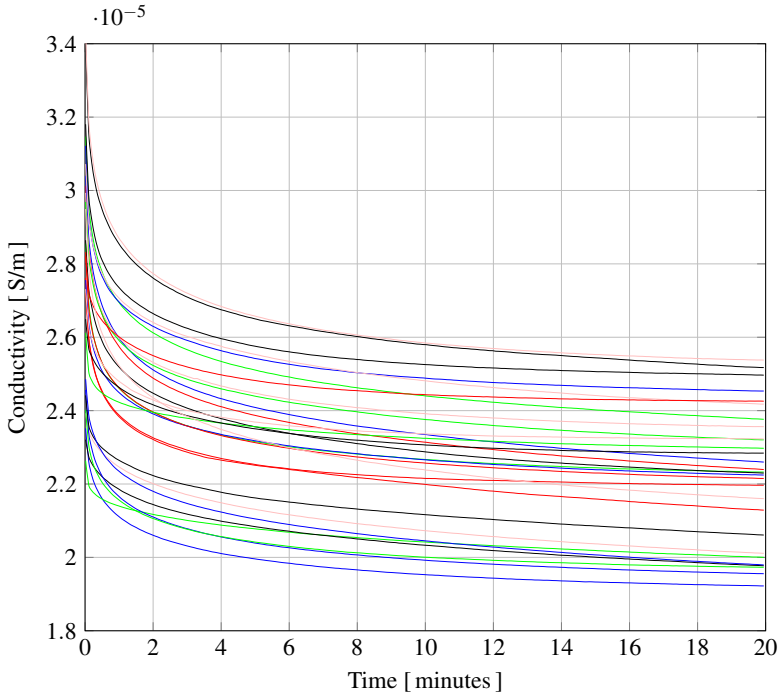

Figure 34: The conductivity of 30 measurements.

Unfortunately the sample height measurement still suffers from noise even for the final design of the test cell. When the adjustable parallels were used, they invariably disturbed the electrode, sometimes even visibly, causing it to shift slightly. This combined with the fact that the electrode is never standing perfectly straight, it is always leaning slightly to one side, creates

problems when measuring the sample height.

The variation in the measured sample height is between 1.965 - 2.32 mm and in Figure 35 the conductivity is plotted against the final value of the conductivity. It is apparent that the sample height measurement is still subjected to noise. If the material was linear, a straight horizontal line would be expected, however, since SiC is non-linear the conductivity should decrease with increasing sample height, this is not observed. The line shown in Figure 35 is a first degree least squares fit and it shows the direct opposite.

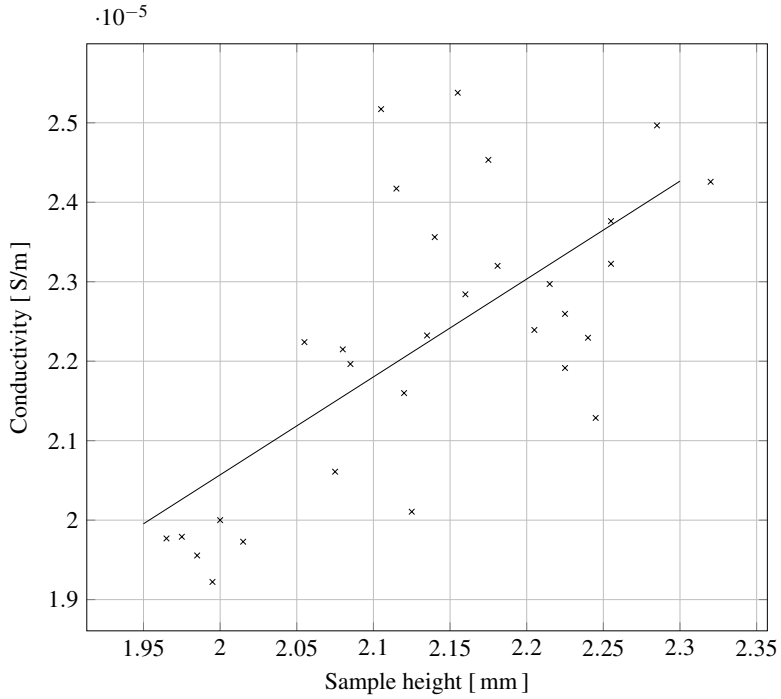

Figure 35: The final measured value of conductivity at different sample heights

The measurements are still very sensitive to physical disturbances. Figures 36 and 37 show what happens when a pair of pliers, (yellow-black, right hand side of the table), which were present at the beginning of the measurement, are very carefully removed from the table. This results in a mechanical disturbance that causes the electrode to shift slightly and the current shape is distorted.

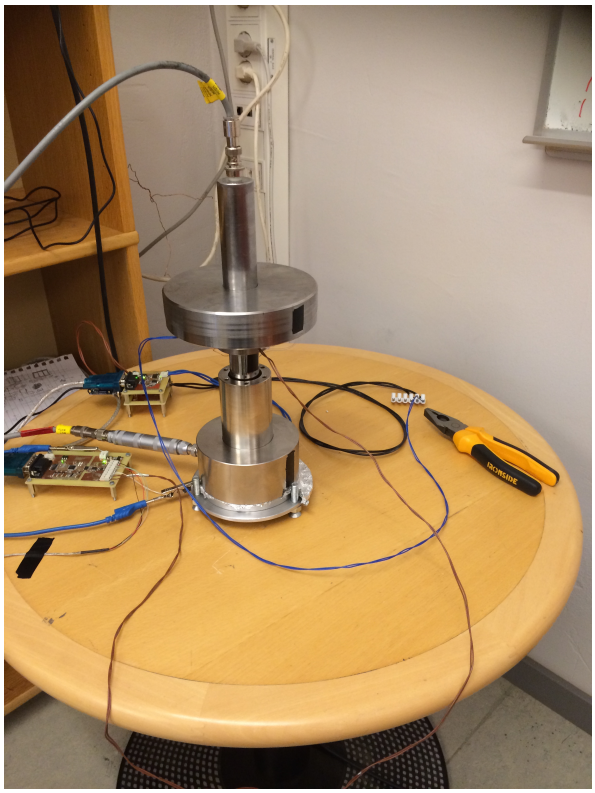

Figure 36: The pliers.

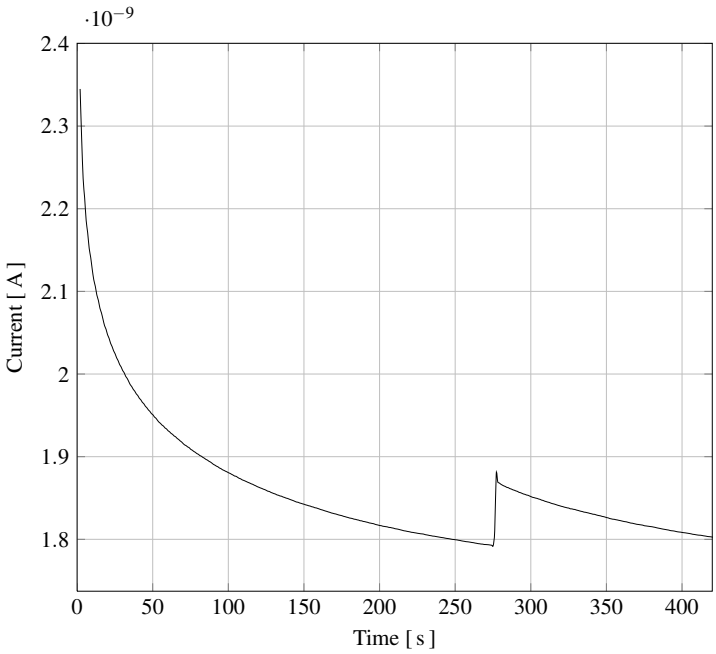

Figure 37: The pliers are removed at 275 seconds.

5 Conclusion

The silicon carbide powder analyzed in this work is used as a part of high voltage accessories where the final conductivity of the product is of interest. Indications from the industry are that the measurements of the conductivity of the final product varies on a significantly larger scale than the conductivity measurements resulting from the hardware and methodology developed in this work. Thus, using the results of this work a test cell can be deployed for measurements of the conductivity of the material at the production facility.

The final set up developed in this study yielded the best repeatability of the results and seems to be suitable for such purposes. A few minor modifications would ease the process and perhaps improve the result.

- The electrode and ballast should be lowered using a pulley
- The temperature control should be separated from the measurement control, allowing pen, paper and a stopwatch to be used instead of computer software to conduct measurements
- The cell should be firmly fastened on a free standing metal support and adjusted using an engineer's spirit level

As shown, the measurements are sensitive and with or without the modifications suggested above they still require meticulous preparation and execution to achieve a usable result. As a consequence of this, the repeatability is basically defined by how well the operator can replicate the conditions for each measurement, specifically concerning sample preparation and electrode insertion. If this system is to be deployed, it would be preferable if the measurements are carried out by a single operator who begins by practicing conducting measurements. When results converge with an acceptable repeatability the project of correlating the measured values of the conductivity of the powder with that of the finished product can begin. At least initially, it might be prudent to carry out several measurements of each individual batch. Care should be afforded to where the sample is taken as there could be distributed variations in conductivity across a produced material.

If better repeatability or if lessening the complexity of conducting measurements is desired, a new system should be constructed. One approach that does both would be to use one or more linear bearings to hold the upper electrode. This would enable simple and accurate measurement of both the sample height using a linear encoder and the force applied using strain gages placed on the sides of the electrode. An important feature of this system is that the upper electrode will be parallel to the lower electrode even when it is used to apply force to the powder.

Recalling the problems caused by using a spring to apply pressure, this subject could be revisited, a more rigid spring could be the solution, or the electrode could be made with enough material to apply sufficient pressure. A third alternative would be to apply hydraulic pressure. If the electrode is lowered with the use of an electric actuator, this should result in improved repeatability. The strain gages should be used to verify that the force is equal and stable in every measurement. This entire structure should be placed in an enclosure that is temperature controlled. If all of the above is constructed successfully, the only variable left is sample preparation. The current way described should at least be tried and evaluated. If all other variables are stable and the sample preparation is deemed to introduce variations, some form of automated processing should be attempted. Instead of using blunt force applied by the operator the process

should be automated. One way of doing that is to inserted the weighed sample into a container whose base consists of the the two lower electrodes in a three electrode system and subject it to well defined vibrations for a given time. Depending on the magnitude of the vibrations the container may have to be sealed. When done it is placed with the use of mechanical guides below the electrode.

Such a system removes all human induced factors from the measurements and should produce results with better repeatability.

References

[1] E. Kuffel, W. S. Zaengl and J. Kuffel, Non-destructive insulation test techniques, High Voltage Engineering: Fundamentals, 2nd ed. Oxford, England: Newnes, 2003, ch.7, sec 1, pp. 395-411.

[2] E. H Rhoderick and R. H. Williams: Metal-Semiconductor contacts, 2nd ed. Oxford, England: Clarendon 1988, ch. 1, sec. 1, pp. 514-546

[3] E. Mårtensson, U. Gäfvert and C. Önneby: “Alternate current characteristics of SiC powders”, J. Appl. Phys. 90, 2870 (2001)

[4] A.K. Jonscher, "Dielectric relaxation in solids", Chelsea Dielectric Press, London 1983.

[5] E. Mårtensson, U. Gäfvert and U.Lindefelt: “Direct current conduction in SiC powders”, J. Appl. Phys. 90, 2862 (2001)

A Measurement schematic and board layout

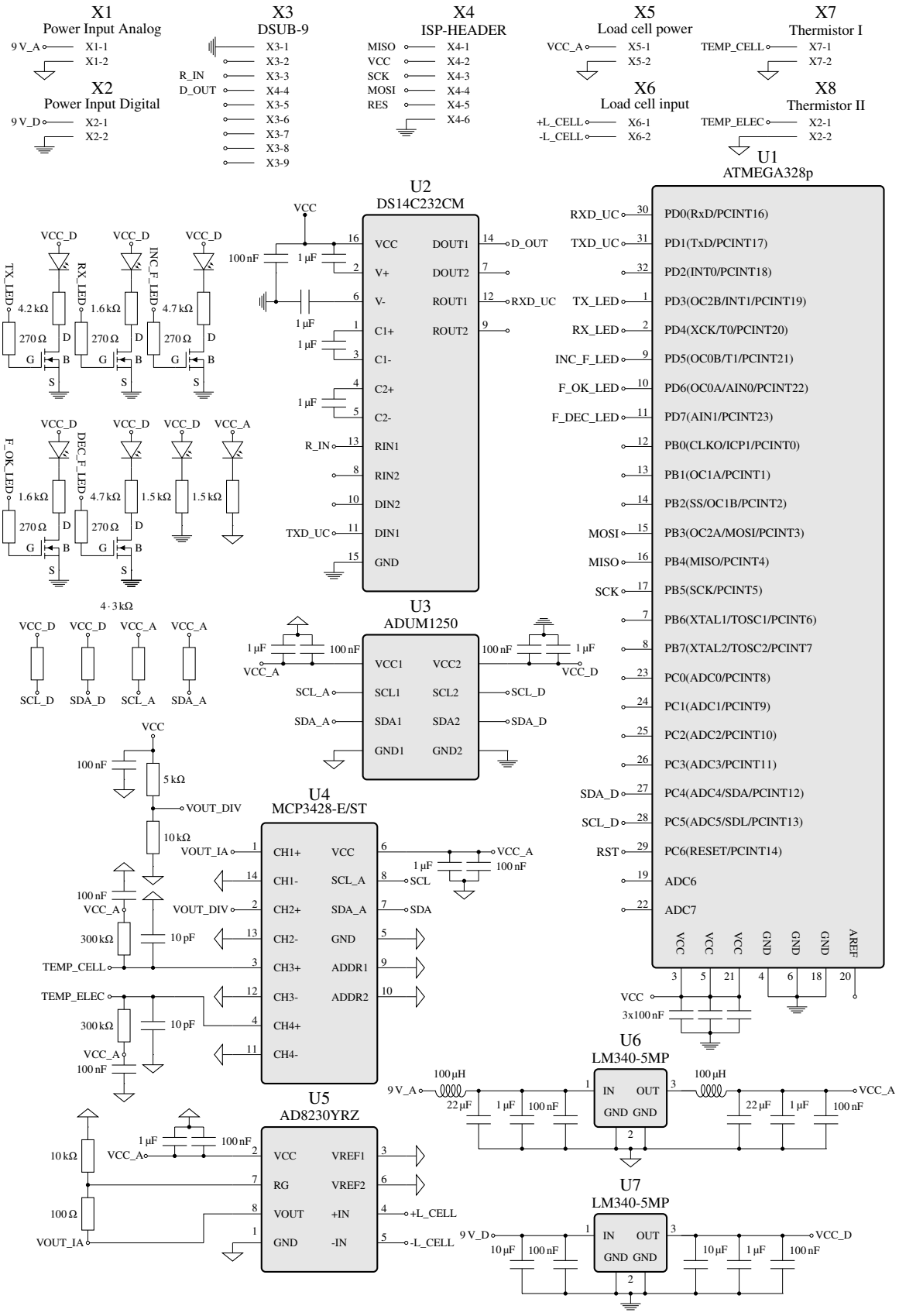

Figure 38: Schematic of the measurement circuitry.

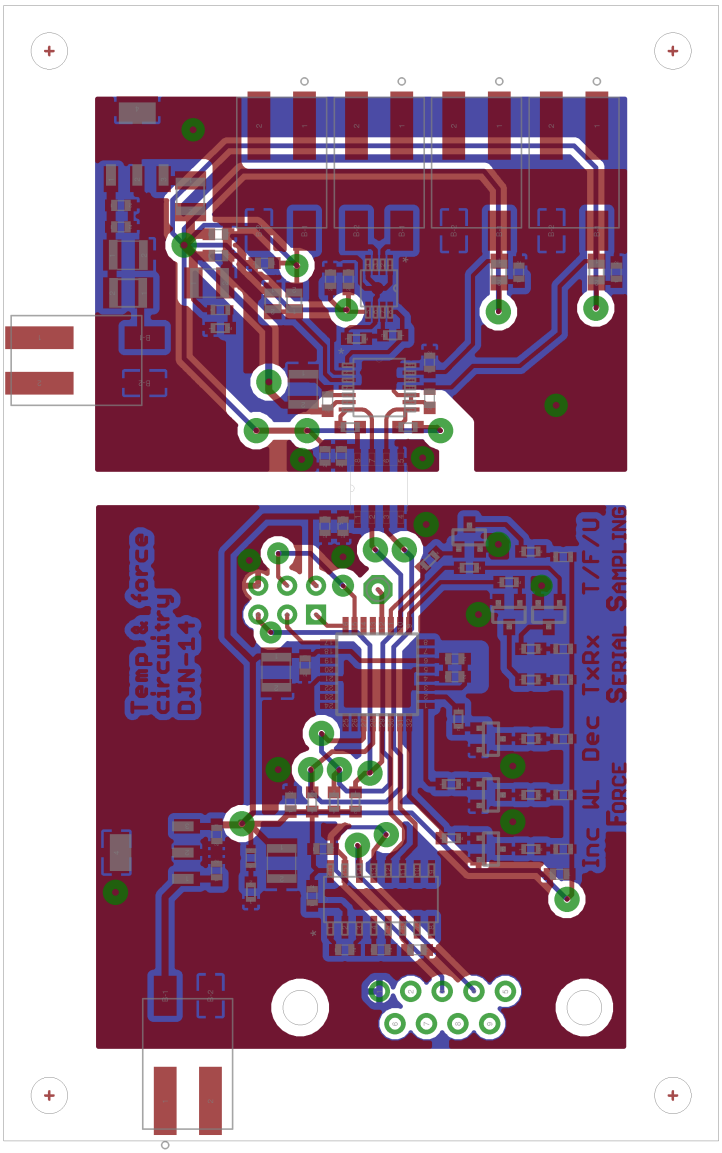

Figure 39: Board layout of the measurement circuitry.

B Heating schematic and board layout

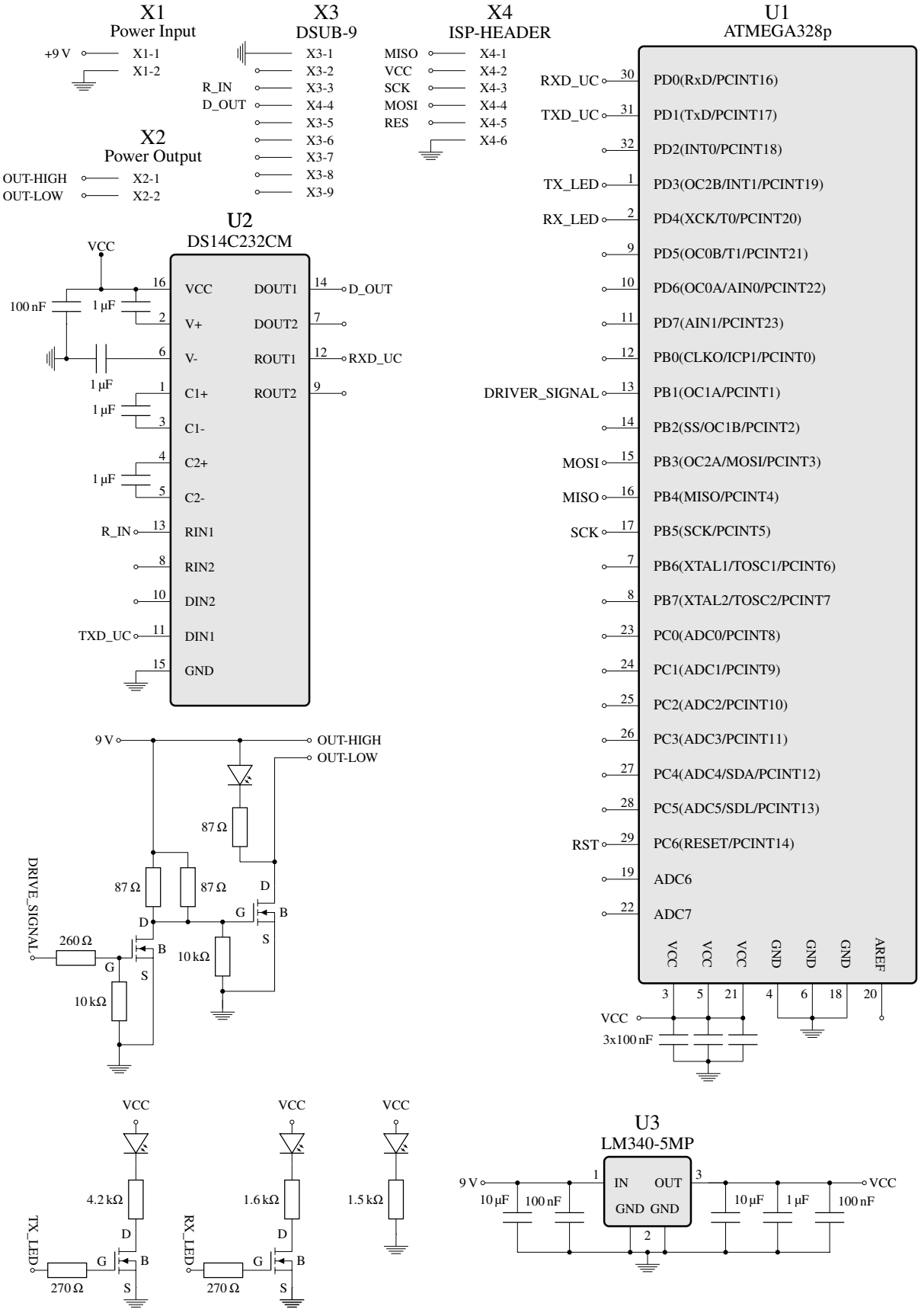

Figure 40: Schematic of the heating circuitry.

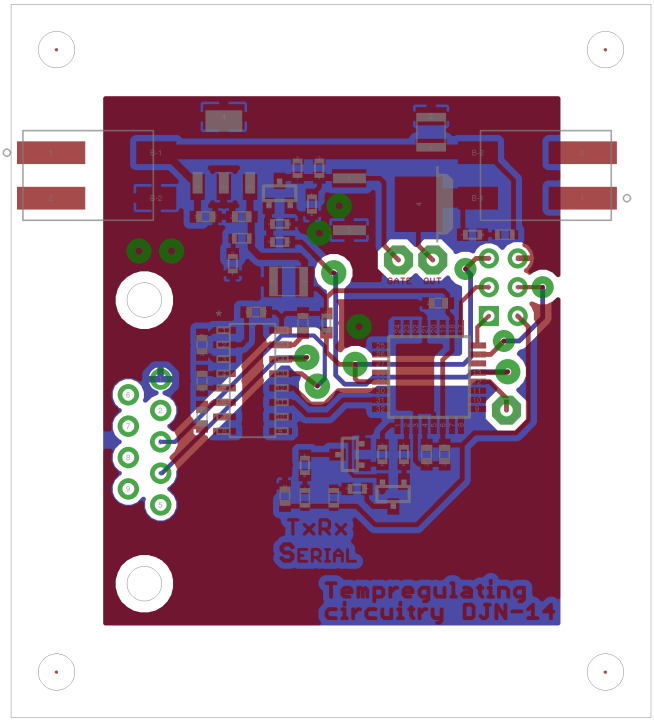

Figure 41: Board layout of the heating circuitry.

C Controlling software

The software that runs the measurement system is written in C and executed on a Linux computer. Communication with the GPIB-Ethernet interface is implemented on the socket layer. Both heating modules and the measurement module are connected via USB and the software maps the system by inquiring each active port what is connected to it and the hardware responds accordingly. The user configures the measurement through a command line interface with the help of a series of questions, such as voltage, time and sampling frequency, it then starts the measurement and logs the information. The measurement electronics continuously transmits information to the computer and the PID-regulators are updated via timers, they start regulating as soon as the program is started. The program waits until both temperatures are within a permitted interval before starting the measurement. Figure 42 shows the flow of information in the system and Figure 43 shows how the measurement interface looks.

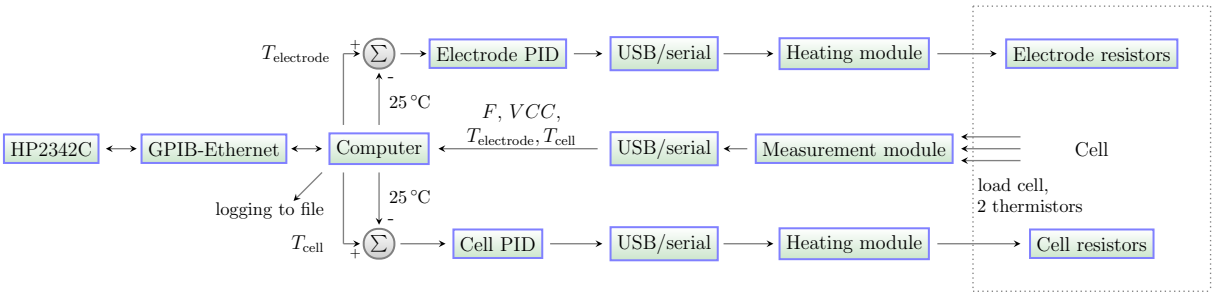

Figure 42: Overview of the measurement system.

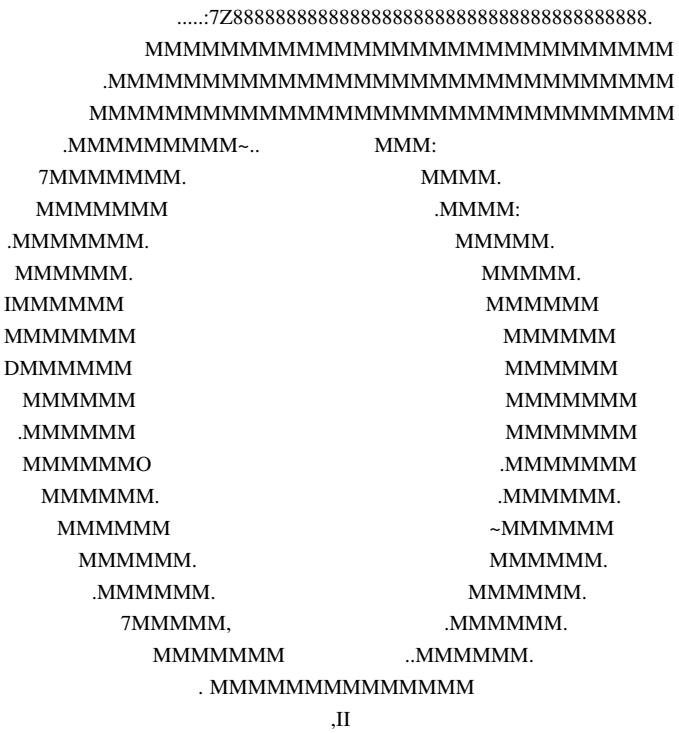

Initializing connection with the GPIB-Ethernet interface
Creating a socket... [ok]
Trying 192.168.0.154... [ok]

Initializing serial interfaces
Found cell heating module on /dev/ttyUSB1 [ok]
Found electrode heating module on /dev/ttyUSB0 [ok]
Found measurement module on /dev/ttyUSB2 [ok]

Configure the measurement, enter the number of your choice
Beware! No checks are done on what is entered, type carefully
(1) - Static voltage, no logging of the off current
(2) - Static voltage, logging of the off current
(3) - Multiple measurements, each with a voltage level and time
(4) - DC-extended - A, (ramp) sample_time != update_time
(5) - DC-extended - B, (ramp)
(6) - Half period sinusoidal
(7) - Arbitrary square waves
(8) - View serial output
(9) - Restart process
(10) - Set PID-parameters for heating
(12) - Enable heating
(13) - Disable heating
(14) - 1 V static with ramp until overcurrent at the end
(0) - Exit
Choice:

Figure 43: An illustration of the measurement interface.